9200 *Inorg. Chem.* **2010**, *49*, 9200–9211
DOI: 10.1021/ic100668b

Inorganic Chemistry
Article

Probing the Antioxidant Action of Selenium and Sulfur Using Cu(I)-Chalcogenone Tris(pyrazolyl)methane and -borate Complexes

Martin M. Kimani, Julia L. Brumaghim,* and Don VanDerveer

Department of Chemistry, Clemson University, Clemson, South Carolina 29634

Received April 8, 2010

Hydroxyl radical generated from the reaction of Cu^+ with hydrogen peroxide results in oxidative DNA damage, and this damage is implicated in aging, cancer, and many other diseases. Selenium- and sulfur-containing compounds can act as antioxidants, and coordination of selenium and sulfur to copper is one explanation for this antioxidant activity. To determine how copper coordination results in antioxidant activity, biologically relevant tris(pyrazolyl)methane and borate Cu^+ complexes of the formulas Tp*Cu(L) and $[Tpm^RCu(L)]^+$, where (L = *N, N*′-dimethylimidazole selone, dmise; *N, N*′-dimethylimidazole thione, dmit; Tp* = hydrotris(3,5-dimethylpyrazolyl)borate; Tpm^R = tris-(pyrazolyl)methane, R = H; Tpm, R = Me; Tpm*, R = *i*Pr; Tpm^{iPr}), have been synthesized and characterized. The structures of complexes Tp*Cu(Dmit), Tp*Cu(dmise), $[Tpm^RCu(dmise)][BF_4]$, and $[Tpm^RCu(Dmit)][BF_4]$ (where R = H; Tpm, R = Me; Tpm*, R = *i*Pr; Tpm^{iPr}) were determined by X-ray crystallography. All the Cu^+ centers adopt distorted tetrahedral coordination geometry, and Cu−Se and Cu−S distances for all the complexes are approximately 2.30 Å, and 2.20 Å, respectively. The effects of counterion and steric bulk at the 3 and 5 positions of the pyrazolyl ring on the structural and spectroscopic properties are discussed. Selone or thione coordination to copper significantly alters the $Cu^{+/2+}$ redox potential: Cu-selone complexes have $Cu^{2+/+}$ potentials from −283 to −390 mV, whereas those of Cu-thione complexes range from 70 to −232 mV versus NHE. The Cu-selone complexes have $Cu^{2+/+}$ potentials near or below that of the cellular reductant NADH (−324 mV). Thus, selenium and sulfur coordination to copper in biological systems may prevent the Cu^{2+} reduction by NADH required for the catalytic formation of damaging hydroxyl radical.

Introduction

Reactive oxygen species (ROS), which include superoxide ($O_2^{\bullet-}$), hydrogen peroxide (H_2O_2), hydroxyl radical ($^{\bullet}OH$), singlet oxygen ($^1O_2^{\bullet}$), and peroxyl radical ($RO_2^{\bullet}$), are involved in oxidative damage to lipids, proteins, and DNA.[1] Copper(I) participates in the Fenton-like reaction (reaction 1) in which hydroxyl radical is generated from the reduction of less-damaging hydrogen peroxide.[2] This copper-mediated hydroxyl radical generation is catalytic in vivo if cellular reductants, such as NADH are available to reduce Cu^{2+} to Cu^+. Numerous studies have linked damage from copper-generated hydroxyl radical to Alzheimer's disease, cardiovascular diseases, and cancer.[3,4]

$$Cu^+ + H_2O_2 \rightarrow Cu^{2+} + HO^{\bullet} + OH^- \qquad (1)$$

Selenium- and sulfur-containing compounds have been widely studied as potential antioxidants for the prevention or reduction of oxidative DNA damage.[5] Selenium is an essential micronutrient for both humans and animals, with a recommended dietary allowance ranging from 55 to 350 μg/day.[6] Organoselenium compounds are of particular interest because they appear to be more bioavailable relative to inorganic selenium compounds.[7]

Using copper-mediated DNA damage studies and UV−vis spectroscopy, our group has identified copper coordination as an explanation for selenium and sulfur antioxidant activity.[5,8−10] This novel metal binding antioxidant hypothesis is separate from the traditional explanation that focuses on the ability of selenium compounds to decompose hydrogen peroxide in a manner similar to glutathione peroxidase (GPx).[11]

*To whom correspondence should be addressed. E-mail: brumagh@clemson.edu.

(1) Honglain, S.; Laurie, G. H.; Ke, J. L. *Free Radical Biol. Med.* **2004**, *37*, 582–593.
(2) Stohs, S. J.; Bagchi, D. *Free Radical Biol. Med.* **1995**, *18*, 321–336.
(3) De Flora, S.; Izzotti, A. *Mutat. Res., Fundam. Mol. Mech. Mutagen.* **2007**, *621*, 5–17.
(4) Evans, M. D.; Dizdaroglu, M.; Cooke, M. S. *Mutat. Res., Rev. Mutat. Res.* **2004**, *567*, 1–61.
(5) Battin, E. E.; Brumaghim, J. L. *Cell Biochem. Biophys.* **2009**, *55*, 1–23.
(6) Schrauzer, G. N. *J. Am. Coll. Nutr.* **2001**, *20*, 1–4.
(7) Tapiero, H.; Townsend, D. M.; Tew, K. D. *Biomed. Pharmacother.* **2003**, *57*, 134–144.
(8) Battin, E. E.; Perron, N. R.; Brumaghim, J. L. *Inorg. Chem.* **2006**, *45*, 499–501.
(9) Ramoutar, R. R.; Brumaghim, J. L. *J. Inorg. Biochem.* **2007**, *101*, 1028–1035.
(10) Battin, E. E.; Brumaghim, J. L. *J. Inorg. Biochem.* **2008**, *102*, 2036–2042.
(11) Mugesh, G.; Singh, H. B. *Chem. Soc. Rev.* **2000**, *29*, 347–357.

Published on Web 09/13/2010

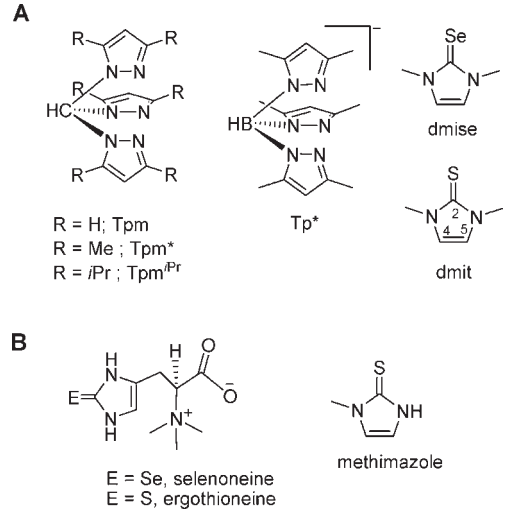

Figure 1. (A) Tris(pyrazolyl) and heterocyclic thione and selone ligands used in this study. Numbering scheme is shown for dmit. (B) Structures of naturally occurring selone and thione antioxidants and the drug methimazole.

As part of our efforts to understand the role of Se/S−Cu coordination in the prevention of metal-mediated DNA damage, biologically relevant Cu^{+} selone and thione complexes with tris(pyrazolyl)methane or tris(pyrazolyl)borate ligands have been synthesized, with the aim of studying their copper coordination and electrochemistry. Scorpionate nitrogen donor ligands first introduced by Trofimenko[12] (Figure 1A) were employed, since they mimic biological coordination.[13] The heterocyclic selones and thiones used in this study (Figure 1A) resemble methimazole, a drug currently used in the treatment of hyperthyroidism (Figure 1B).[14] Dmit and dmise are also structurally similar to ergothioneine,[15] and selenoneine,[16] respectively, antioxidant compounds widely found in plant and animal tissues (Figure 1B).

The heterocyclic chalcogenones used in this study are good σ- and π-donors, and similar compounds, such as imidazoline-2-thiones, display a diversity of bonding modes.[17] The coordination chemistry of selones and thiones with transition metals and halogens has been previously reviewed by Raper,[18] Akrivos,[19] Spicer et al.,[20] and Pettinari,[21] as well as studied by Devillanova et al.,[22] Williams et al.,[23−27] Rabinovich et al.,[28,29] and Parkin et al.[30,31] Many reports describe the coordination chemistry of thiones with Cu^{+},[17,32−35] but reports of analogous selone complexes are few.[36−38] Herein, we report the synthesis and characterization of mononuclear, four coordinate-copper(I) complexes: Tp*-Cu(L) and $[Tpm^{R}Cu(L)]^{+}$ where (L = *N,N′*-dimethylimidazole selone, dmise; *N,N′*-dimethylimidazole thione, dmit; Tp* = hydrotris(3,5-dimethylpyrazolyl)borate; Tpm^{R} = tris(pyrazolyl)methane, R = H; Tpm, R = Me; Tpm*, R = *i*Pr; Tpm^{iPr}). Brumaghim et al.[8,10,39] and others[40] have determined that the antioxidant activities of analogous selenium and sulfur compounds can be very distinct. Thus, we have investigated the geometries and spectroscopic properties of both copper-selone and -thione complexes. Because selenium and sulfur coordination to copper is necessary for prevention of copper mediated DNA damage, comparative electrochemical studies of selone and thione complexes will help determine changes in the reduction potentials of $Cu^{2+/+}$ upon coordination. These comparative studies will provide insights into the effects of selenium and sulfur coordination and antioxidant activity in vivo.

Experimental Section

Materials. The synthesis and manipulation of all copper complexes was performed under an inert atmosphere of argon or nitrogen using standard Schlenk techniques. Acetonitrile, methanol, and ether were purified using standard procedures and freshly distilled under argon atmosphere prior to use. The following compounds were synthesized according to published procedures: 3,5-diisopropyl pyrazole,[41] hydrotris(3,5-diisopropyl-1-pyrazoyl)methane (Tpm^{iPr}),[42] potassium hydro-tris(3,5-dimethylpyrazolyl)borate (Tp*),[43] *N,N′*-dimethylimidazole

(12) Trofimenko, S. *Chem. Rev.* **1993**, *93*, 943–980.
(13) Field, D. L.; Messerle, B. A.; Soler, L. P.; Hambley, T. W.; Turner, P. *J. Organomet. Chem.* **2002**, *655*, 146–157.
(14) Cooper, D. S. *N. Engl. J. Med.* **2005**, *352*, 905–917.
(15) Ey, J.; Schomig, E.; Taubert, D. *J. Agric. Food Chem.* **2007**, *55*, 6466–6474.
(16) Yamashita, Y.; Yamashita, M. *J. Biol. Chem.* **2010**, *285*, 18134–18138.
(17) Lobana, T. S.; Sharma, R.; Butcher, R. J. *Z. Anorg. Allg. Chem.* **2008**, *634*, 1785–1790.
(18) Raper, E. S. *Coord. Chem. Rev.* **1985**, *61*, 115–184.
(19) Akrivos, P. D. *Coord. Chem. Rev.* **2001**, *213*, 181–210.
(20) Spicer, M. D.; Reglinski, J. *Eur. J. Inorg. Chem.* **2009**, 1553–1574.
(21) Pattinari, C. *Scorpionates II: Chelating Borate Ligands, Dedicated to Swiatoslaw Trofimenko*; Imperial College Press: London, 2008; pp 381−415.
(22) Bigoli, F.; Demartin, F.; Deplano, P.; Devillanova, F. A.; Isaia, F.; Lippolis, V.; Mercuri, M. L.; Pellinghelli, M. A.; Trogu, E. F. *Inorg. Chem.* **1996**, *35*, 3194–3201.
(23) Williams, D. J.; McKinney, B. J.; Baker, B.; Gwaltney, K. P.; VanDerveer, D. *J. Chem. Crystallogr.* **2007**, *37*, 691–694.
(24) Williams, J. D.; Concepcion, J. J.; Koether, M. C.; Arrowood, A. K.; Carmack, A. L.; Hamilton, T. G.; Luck, S. M.; Ndomo, M.; Teel, R. C.; VanDerveer, D. *J. Chem. Crystallogr.* **2006**, *36*, 453–457.
(25) Williams, D. J.; White, K. M.; VanDerveer, D.; Wilkinson, A. P. *Inorg. Chem. Commun.* **2002**, *5*, 124–126.
(26) Williams, D. J.; Jones, T. A.; Rice, E. D.; Davis, K. J.; Ritchie, J. A.; Pennington, W. T.; Schimek, G. L. *Acta Crystallogr., Sect. C: Cryst. Struct. Commun.* **1997**, *53*, 837–838.
(27) Williams, D. J.; Fawcett, M. R. B.; Raye, R. R.; VanDerveer, D.; Pang, Y. T.; Jones, R. L.; Bergbauer, L. K. *Heteroat. Chem.* **1993**, *4*, 409–413.
(28) Patel, D. V.; Mihalcik, D. J.; Kreisel, K. A.; Yap, G. P.; Zakharov, L. N.; Kassel, W. S.; Rheingold, A. L.; Rabinovich, D. *Dalton Trans.* **2005**, 2410–2416.
(29) Maffett, L. S.; Gunter, K. L.; Kreisel, K. A.; Yap, G. P. A.; Rabinovich, D. *Polyhedron* **2007**, *26*, 4758–4764.
(30) Landry, V. K.; Buccella, D.; Pang, K. L.; Parkin, G. *Dalton Trans.* **2007**, 866–870.
(31) Parkin, G. *New J. Chem.* **2007**, *31*, 1996–2014.
(32) Lobana, T. S.; Sultana, R.; Hundal, G. *Polyhedron* **2008**, *27*, 1008–1016.
(33) Lobana, T. S.; Castineiras, A. *Polyhedron* **2002**, *21*, 1603–1611.
(34) Aslanidis, P.; Hadjikakou, S. K.; Karagiannidis, P.; Cox, P. J. *Inorg. Chim. Acta* **1998**, *271*, 243–247.
(35) Kim, H. R.; Jung, I. G.; Yoo, K.; Jang, K.; Lee, E. S.; Yun, J.; Son, S. U. *Chem. Commun.* **2010**, *46*, 758–760.
(36) Devillanova, F. A.; Diaz, A.; Isaia, F.; Verani, G. *Transition Met. Chem.* **1989**, *14*, 153–154.
(37) Blake, A. J.; Lippolis, V.; Pivetta, T.; Verani, G. *Acta. Crystallogr., Sect. C* **2007**, *63*, m364–367.
(38) Minoura, M.; Landry, V. K.; Melnick, J. G.; Pang, K. L.; Marchio, L.; Parkin, G. *Chem. Commun.* **2006**, 3990–3992.
(39) Battin, E. E.; Ramoutar, R. R.; Quarles, C.; Zimmerman, M. T.; Brumaghim, J. L., manuscript in preparation.
(40) Collins, C. A.; Fry, F. H.; Holme, A. L.; Yiakouvaki, A.; Al-Qenaei, A.; Pourzand, C.; Jacob, C. *Org. Biomol. Chem.* **2005**, *3*, 1541–1546.
(41) Kitajima, N.; Fujisawa, K.; Fujimoto, C.; Moro-oka, Y.; Hashimoto, S.; Kitagawa, T.; Toriumi, K.; Nakamura, A. *J. Am. Chem. Soc.* **1992**, *114*, 1277–1291.
(42) Fujisawa, K.; Ono, T.; Ishikawa, Y.; Amir, N.; Miyashita, Y.; Okamoto, K.; Lehnert, N. *Inorg. Chem.* **2006**, *45*, 1698–1713.
(43) Trofimenko, S. *J. Am. Chem. Soc.* **1967**, *89*, 3170–3177.

selone (dmise), *N*,*N*′-dimethylimidazole thione (dmit),[44] $[Cu(NCCH_3)_4][BF_4]$,[45] Tpm*CuCl, $[Tpm*Cu(NCCH_3)]^+$,[46] hydrotris(3,5-dimethyl-1-pyrazoyl)methane (Tpm*),[47] Tpm^{iPr}-CuCl and $[Tpm^{iPr}Cu(NCCH_3)]^+$.[42] The following reagents were used as received: cuprous chloride (Aldrich), 3,5-dimethyl-1-pyrazole (Aldrich), tetra-*n*-butylammonium bromide (Aldrich), sodium carbonate (VWR), selenium powder (Alfa Aesar), sulfur powder (Alfa Aesar), cuprous oxide (stabilized; Aldrich), diisobutyrylmethane (VWR), hydrazine monohydrate (VWR), 1-methylimidazole (VWR), and methyliodide (VWR).

Instrumentation. ^1H, ^{13}C, and ^{19}F NMR spectra were obtained on Bruker-AVANCE 300 and 500 MHz NMR spectrometers. ^{11}B NMR spectra were obtained on a Joel 300 MHz NMR spectrometer. ^1H and ^{13}C NMR chemical shifts are reported in δ relative to tetramethylsilane (TMS) and referenced to solvent. ^{19}F NMR and ^{11}B NMR spectra were externally referenced to CCl_3F (δ 0)[48] and neat $BF_3 \cdot OEt_2$ (δ −19.4),[49] respectively.

Electrochemical experiments were performed with a BAS 100B potentiostat. A three compartment cell was used with an Ag/AgCl reference electrode, Pt counter electrode, and a glassy carbon working electrode. Freshly distilled acetonitrile was used as the solvent with tetra-*n*-butylammonium phosphate as the supporting electrolyte (0.1 M). Solutions containing 1 mmol analyte were deaerated for 2 min by vigorous nitrogen purge. The measured potentials were corrected for junction potentials relative to ferrocenium/ferrocene (0.543 mV vs Ag/AgCl).[50] All $E_{1/2}$ values were calculated from $(E_{pa} + E_{pc})/2$ at a scan rate of 100 mV/s, and $\Delta E = E_{pa} - E_{pc}$. Cyclic voltammograms of selone and thione ligands and their copper complexes showing the $Cu^{+/2+}$ potentials are given in Figures S3−S5 of the Supporting Information. Resistivity for each complex was measured in DMF solution (0.1 mM) at 25 °C using a GDT-11 multimeter and converted to molar electrical conductivity.

Infrared spectra were obtained using Nujol mulls on KBr salt plates with a Magna 550 IR spectrometer. Abbreviations used in the description of vibrational data are as follows: vs, very strong; s, strong; m, medium; w, weak; b, broad. Electrospray ionization mass spectrometry (ESI-MS) was conducted using a QSTAR XL Hybrid MS/MS System from Applied Biosystems via direct injection of sample (0.05 mL/min flow rate) into a Turbo Ionspray ionization source. Samples were run under positive mode, with ionspray voltage of 5500 V, and TOF scan mode. Melting points were determined using a Barnstead Electrothermal 9100 apparatus in silicon-grease-sealed glass capillary tubes. Absorption spectra were collected using a Varian Cary-50 Bio spectrophotometer in quartz cuvettes with a path length of 1 cm. Elemental analysis was performed by Atlantic Microlabs, Inc.

Preparation of Complexes. [Tpm*Cu(dmise)][BF$_4$] (1). Method 1. The dmise ligand (176 mg, 1 mmol) was dissolved in acetonitrile (20 mL) and was cannula transferred into a solution of $[Cu(CNCH_3)_4][BF_4]$ (312 mg, 1 mmol) in acetonitrile (20 mL). The reaction mixture was stirred at room temperature for 3 h until it was clear and colorless. An equimolar amount of Tpm* (298 mg, 1 mmol) was then dissolved in acetonitrile (10 mL) and cannula transferred into the reaction mixture and stirred for an additional 18 h. The solvent volume in the reaction mixture was reduced to about 4 mL, and the product was precipitated with diethyl ether to afford an off-white solid that was dried in vacuo and analyzed. Yield 78% (486 mg, 0.78 mmol).

Method 2. $[Tpm*Cu(NCCH_3)][BF_4]$[46] (250 mg, 0.5 mmol) was dissolved in dichloromethane (10 mL), and into this was cannula transferred dmise (90 mg, 0.5 mmol) in dichloromethane (10 mL). The reaction mixture was stirred for 3 h, and the solvent volume reduced to about 3 mL. The product was precipitated with diethyl ether to afford an off-white solid that was dried in vacuo and analyzed. Single crystals for X-ray analysis were grown from slow vapor diffusion of ether into acetonitrile solution. Yield: 89% (277 mg, 0.445 mmol). ^1H NMR (CD_2Cl_2): 2.18 (s, 9H, $3CH_3$), 2.541 (s, 9H, $3CH_3$), 3.88 (s, 6H, $2CH_3$ [dmise]), 5.99 (s, 3H, 3CH [Pz]), 7.17 (s, 2H, 2CH [dmise]), 7.77 (s, 1H, CH). $^{13}C\{^1H\}$ NMR (CD_2Cl_2): 10.72 (CH_3), 13.16 (CH_3), 37.58 (CH_3 [dmise], 67.86 (CH), 106.76 (C-4 [Pz]), 121.60 (2CH [dmise]), 139.60 (C-3 [Pz]), 147.61 (C═Se), 150.79 (C-5 [Pz]). $^{19}F\{^1H\}$ NMR: −152.46, −152.52 (s, $^{10}BF_4$, $^{11}BF_4$). $^{11}B\{^1H\}$ NMR (CD_3CN): −1.397. IR (cm^{-1}): 481 s, 520 vs, 582 s, 610 s, 630 vs, 661 vs, 703 s, 739 vs, 793 vs, 815 s, 853 w, 900 vs, 980 s, 1031 b, 1150 vs, 1239 b, 1306 w, 1454 w, 1569 s, 1688 s, 2362 s, 2722 s, 3141 s, 3171 s, 3423 b. UV−vis (CH_3CN): 273 nm. Melting point (Mp): 169−172 °C. Mass spectrum (ESI-MS): *m*/*z* 537.1 $[Tpm*Cu(dmise)]^+$, 361.1 $[Tpm*Cu]^+$. Molar conductivity: 90.42 S cm^2 mol^{-1}. Anal. Calcd for $C_{21}H_{30}BCuF_4N_8Se$: C, 40.43; N, 17.96; H, 4.86. Found: C, 40.19; N, 17.74; H, 4.84.

[Tpm*Cu(dmit)][BF$_4$] (2). Complex **2** was prepared following the procedure for **1** using both methods except that dmit (1 mmol, 129 mg) was used in place of dmise. Yield: method 1, 64% (368 mg, 0.640 mmol); method 2, 78% (451 mg, 0.780 mmol). Single crystals for X-ray analysis were grown from slow vapor diffusion of ether into acetonitrile solution. ^1H NMR (CD_2Cl_2): 2.18 (s, 9H, $3CH_3$), 2.53 (s, 9H, $3CH_3$), 3.80 (s, 6H, $2CH_3$ [dmit]), 6.00 (s, 3H, 3CH [Pz]), 7.00 (s, 2H, 2CH [dmit]), 7.76 (s, 1H, CH). $^{13}C\{^1H\}$ NMR: 10.72 (CH_3), 13.11 (CH_3), 35.82 (CH_3 [dmit]), 67.79 (CH), 106.74 (C-4 [Pz]), 119.70 (2CH [dmit]), 139.58 (C-3 [Pz]), 150.78 (C-5 [Pz]), 155.96 (C═S). $^{19}F\{^1H\}$ NMR: −152.56, 152.61 (s, $^{10}BF_4$, $^{11}BF_4$). $^{11}B\{^1H\}$ NMR (CD_3CN): −1.43. IR (cm^{-1}): 481 s, 520 s, 582 s, 611 m, 630 vs, 672 vs, 703 s, 734 vs, 751 vs, 795 m, 816 s, 854 m, 900 vs, 976 s, 1058 b, 1149 vs, 1171 vs, 1239 m, 1306 s, 1393 b, 1570 s, 1676 s, 2723 s, 3141 vs, 3171 vs, 3351 w. UV−vis (CH_3CN): 273 nm. Mp: 167−170 °C. Mass spectrum (ESI-MS): *m*/*z* 489.1 $[Tpm*Cu(dmit)]^+$, 361.1 $[Tpm*Cu]^+$, 319.0 $[Cu\text{-}(dmit)_2]^+$, 191.0 $[Cu\text{-}dmit]^+$. Molar conductivity: 89.74 S cm^2 mol^{-1}. Anal. Calcd for $C_{21}H_{30}BCuF_4N_8S$: C, 43.72; N, 19.42; H, 5.24. Found: C, 43.78; N, 19.36; H, 5.27.

[TpmCu(dmise)][BF$_4$] (3). Complex **3** was prepared following the procedure for **1** using both methods except that Tpm (214 mg, 1 mmol) was used in place of Tpm*. Yield: method 1, 83% (447 mg, 0.83 mmol); method 2, 87% (471 mg, 0.87 mmol). Single crystals for X-ray analysis were grown from slow vapor diffusion of ether into a methanol solution. ^1H NMR (CD_3CN): 3.73 (s, 6H, CH_3 [dmise]), 6.45 (b, 3H, CH [Pz]), 7.15 (s, 2H, CH [dmise]), 7.70 (b, 3H, CH [Pz]), 7.82 (b, 3H, CH [Pz]), 8.66 (s, H, CH). $^{13}C\{^1H\}$ NMR (CD_3CN): 38.02 (CH_3 [dmise]), 81.9 (CH), 107.87 (4-CH [Pz]), 122.24 (2CH [dmise]), 131.71 (3-CH [Pz]), 142.68 (5-CH [Pz]), 148.9 (C═Se). $^{19}F\{^1H\}$ NMR (CD_3CN): −149.557, −149.610 (s, $^{10}BF_4$, $^{11}BF_4$). IR (cm^{-1}): 521 w, 603 w, 611 w, 656 w, 723 s, 761 vs, 799 vs, 815 vs, 917 w, 961 w, 978 w, 1093 b, 1208 w, 1233 s, 1275 s, 1307 vs, 1351 s, 1379 vs, 1396 s, 1458 vs, 1507 s, 1522 s, 1540 w, 1570 w, 1652 w, 1700 w, 2337 w, 2361 w, 2724 w, 2920 b, 3133 b. UV−vis (CH_3CN): 275 nm. Mp: 204−206 °C. Mass spectrum (ESI-MS): *m*/*z* 452.9 $[TpmCu(dmise)]^+$, 277.0 $[TpmCu]^+$. Anal. Calcd for $C_{15}H_{18}BCuF_4N_8Se$: C, 33.38; N, 20.76; H, 3.36. Found: C, 33.17; N, 20.55; H, 3.34.

[TpmCu(dmit)][BF$_4$] (4). Complex **4** was prepared following the procedure for **1** using both methods except that Tpm (214 mg,

(44) Roy, G.; Das, D.; Mugesh, G. *Inorg. Chim. Acta* **2007**, *360*, 303–316.
(45) Kubas, G. J. *Inorg. Synth.* **1990**, *28*, 68–70.
(46) Reger, D. L.; Collins, J. E. *Organometallics* **1996**, *15*, 2029–2032.
(47) Reger, G. L.; Grattan, T. C.; Brown, K. J.; Little, C. A.; Lamba, J. J. S.; Rheingold, A. L.; Sommer, R. D. *J. Organomet. Chem.* **2000**, *607*, 120–128.
(48) Harris, R. K.; Mann, B. E. *NMR and the Periodic Table*; Academic Press: London, 1978; p 99.
(49) Matsuo, H.; Miyazaki, Y.; Takemura, H.; Matsuoka, S.; Sakashita, H.; Yoshimura, K. *Polyhedron* **2004**, *23*, 955–961.
(50) Connelly, N. G.; Geiger, W. E. *Chem. Rev.* **1996**, *96*, 877–910.

1 mmol) and dmit (129 mg, 1 mmol) were used in place of Tpm* and dmise. Yield: method 1, 79% (389 mg, 0.791 mmol); method 2, 75% (368 mg, 0.749 mmol). Single crystals for X-ray analysis were grown from slow vapor diffusion of ether into a methanol solution. ^{1}H NMR (CD_2Cl_2): 3.82 (s, 6H, CH_3 [dmit]), 6.35 (t, J_{HH} = 2 Hz, 3H, CH [Pz]), 7.04 (s, 2H, CH [dmit]), 7.53 (d, J_{HH} = 2 Hz, 3H, CH [Pz]), 8.26 (d, J_{HH} = 2.5 Hz, 3H, CH [Pz]), 9.14 (s, H, CH). ^{13}C{^{1}H} NMR (CD_2Cl_2): 35.93 (CH_3 [dmit]), 76.08 (CH), 106.65 (4-CH [Pz]), 119.90 (2CH [dmit]), 132.07 (3-CH [Pz]), 141.64 (5-CH [Pz]), 154.66 (C=S). ^{19}F{^{1}H} NMR (CD_2Cl_2): −149.557, −149.610 (s, $^{10}BF_4$, $^{11}BF_4$). IR (cm^{-1}): 520 w, 613 vs, 661 w, 671 s, 719 vs, 750 vs, 772 vs, 794 vs, 851 vs, 921 w, 970 s, 1020 b, 1092 b, 1174 s, 1232 s, 1242 vs, 1258 w, 1288 vs, 1307 w, 1377 s, 1400 vs, 1464 vs, 1512 s, 1542 w, 1571 s, 2361 w, 2727 w, 2925 b, 3016 w, 3107 w, 3137 w, 3173 w. Mp: 205−207 °C. UV−vis (CH_3CN): 273 nm. Mass spectrum (ESI-MS): *m*/*z* 405.0 [TpmCu(dmit)]$^+$, 277.0 [TpmCu]$^+$, 191.0 [Cu-dmit]$^+$. Anal. Calcd for $C_{15}H_{18}BCuF_4N_8S$: C, 36.56; N, 22.74; H, 3.68. Found: C, 36.61; N, 22.77; H, 3.63.

[Tpm$^{i\mathrm{Pr}}$Cu(dmit)][BF$_4$] (5). Complex **5** was prepared following the procedure for **1** using both methods except that Tpm$^{i\mathrm{Pr}}$ (466 mg, 1 mmol) and dmit (129 mg, 1 mmol) were used in place of Tpm* and dmise, respectively. Yield: method 1, 83% (617 mg, 0.83 mmol).

Synthesis of complex **5** by method 2 was conducted following procedure for **1**, but with slight modifications. [Tpm$^{i\mathrm{Pr}}$Cu(NCCH$_3$)][BF$_4$][42] (660 mg, 1 mmol) was dissolved in dichloromethane (10 mL), and into this was cannula transferred dmit (128 mg, 1 mmol) in dichloromethane (10 mL). The reaction mixture was stirred for 3 h, and the solvent volume reduced to about 3 mL. The product was extracted with diethyl ether to afford a yellowish solution that was dried in vacuo and analyzed. Yield: 87% (648 mg, 0.872 mmol). Single crystals for X-ray analysis were grown via slow vapor diffusion of ether into dichloromethane solution. ^{1}H NMR (CD_2Cl_2): 1.19 (d, J_{HH} = 7 Hz, 18H, 3(CH_3)$_2$), 1.33 (d, J_{HH} = 7 Hz, 18H, 3(CH_3)$_2$), 2.96 (sept, J_{HH} = 7 Hz, 3H, 3CH), 3.12 (sept, J_{HH} = 6.75 Hz, 3H, 3CH), 3.77 (s, 6H, 2CH_3 [dmit]), 6.05 (s, 3H, 3CH [Pz]), 7.03(s, 2H, 2CH [dmit]), 8.00 (s, 1H, CH). ^{13}C{^{1}H} NMR (CD_2Cl_2): 22.31 (CH(CH_3)$_2$), 22.88 (CH(CH_3)$_2$), 26.18 (CH(CH_3)$_2$), 27.84 (CH(CH_3)$_2$), 35.81 (CH_3 [dmit]), 67.28 (CH), 99.71 (4-CH [Pz]), 119.80 (2CH [dmit]), 150.85 (3-CH [Pz]), 155.49 (C=S), 160.99 (5-CH [Pz]). ^{19}F{^{1}H} NMR (CD_2Cl_2): −152.844, −152.896 (s, $^{10}BF_4$, $^{11}BF_4$). ^{11}B NMR (CD_2Cl_2): −4.69. IR (cm^{-1}): 520 s, 582 s, 633 s, 669 vs, 695 s, 723 s,743 s, 799 s, 821 vs,879 s, 902 s, 914 s, 1005 s, 1053 b, 1180 vs, 1235 vs, 1289 s, 1366 s, 1394 m, 1464 w, 1556 vs, 1569 s,1682 b, 1737 s, 2126 b, 2359 b, 2727 b, 3139 s, 3167 s, 3364 b. Mp: 232 °C. UV−vis (CH_3CN): 261 nm. Mass spectrum (ESI-MS): *m*/*z* 657.2 [Tpm$^{i\mathrm{Pr}}$Cu(dmit)]$^+$, 529.2 [Tpm$^{i\mathrm{Pr}}$Cu]$^+$, 319.0 [Cu-(dmit)$_2$]$^+$, 191.0 [dmit-Cu]$^+$. Molar conductivity: 95.61 S cm^2 mol^{-1}. Anal. Calcd for $C_{33}H_{54}BCuF_4N_8S$: C, 53.23; N, 15.15; H, 7.26. Found: C, 53.44; N, 14.92; H, 7.42.

[Tpm$^{i\mathrm{Pr}}$Cu(dmise)][BF$_4$] (6). Complex **6** was prepared following the procedure for **1** using both methods except that Tpm$^{i\mathrm{Pr}}$ (466 mg, 1 mmol) was used in place of Tpm*. Yield: method 1, 62% (491 mg, 0.619 mmol). Method 2 was modified as stated in procedure for **5**. Yield: 67% (530 mg, 0.67 mmol). Single crystals for X-ray analysis were grown via slow vapor diffusion of ether into dichloromethane solution. ^{1}H NMR (CD_2Cl_2): 1.17 (d, J_{HH} = 7 Hz, 18H, 3(CH_3)$_2$), 1.32 (d, J_{HH} = 7 Hz, 18H, 3(CH_3)$_2$), 2.98 (sept, J_{HH} = 6 Hz, 3H, 3CH), 3.11 (sept, J_{HH} = 6.75 Hz, 3H, 3CH), 3.85 (s, 6H, 2CH_3 [dmise]), 6.04 (s, 3H, 3CH [Pz]), 7.18 (s, 2H, 2CH [dmise]), 8.01 (s, 1H, CH). ^{13}C{^{1}H} NMR (CD_2Cl_2): 22.40 (CH(CH_3)$_2$), 22.87 (CH(CH_3)$_2$), 26.19 (CH(CH_3)$_2$), 27.82 (CH(CH_3)$_2$), 37.57 (CH_3 [dmise]), 67.50 (CH), 99.64 (4-CH [Pz]), 121.47 (2CH [dmise]), 148.12 (C=Se), 150.81(3-CH [Pz]), 161.04(5-CH [Pz]). ^{19}F{^{1}H} NMR (CD_2Cl_2): −152.932, −152.984 (s, $^{10}BF_4$, $^{11}BF_4$). ^{11}B{^{1}H} NMR [(CD_3CN)]: −1.39. IR (cm^{-1}): 520 s, 583 s, 669 vs, 694 s, 723 s, 746 vs, 797 vs, 821 b, 878 s, 902 s, 914 vs, 928 s, 964 s, 1004 s, 1044 b, 1150 s, 1182 s, 1234 b, 1289 b, 1383 b, 1458 b, 1556 s, 1679 s, 2125 s, 2359 s, 2728 s, 3139 s, 3165 s, 3357 b. Mp: 234 °C. UV−vis (CH_3CN): 273 nm. Mass spectrum (ESI-MS): *m*/*z* 705.2 [Tpm$^{i\mathrm{Pr}}$Cu(dmise)]$^+$, 529.2 [Tpm$^{i\mathrm{Pr}}$Cu]$^+$. Molar conductivity: 118.4 S cm^2 mol^{-1}. Anal. Calcd for $C_{33}H_{54}CuN_8SeBF_4$: C, 50.04; N, 14.15; H, 6.87. Found: C, 49.92; N, 14.23; H, 6.99.

Tp*Cu(dmit) (7). Method 1. The dmit ligand (134 mg, 1 mmol) was dissolved in acetonitrile (20 mL) and was cannula transferred into a solution of CuCl (99 mg, 1 mmol) in methanol (20 mL). The reaction mixture was stirred at room temperature for 3 h, and an equimolar amount of KTp* (330 mg, 1 mmol) dissolved in acetonitrile was cannula transferred into the reaction mixture, stirred for 18 h, and dried in vacuo. The target product was extracted using dichloromethane, and the filtrate was dried in vacuo and analyzed. Single crystals suitable for X-ray structure determination were grown by slow diffusion of ether into methanol/dichloromethane solution. Yield 75% (365 mg, 0.75 mmol).

Method 2. [Tp*Cu(NCCH$_3$)] (200 mg, 0.5 mmol) was dissolved in dichloromethane (10 mL), and dmit (90 mg, 0.5 mmol) in dichloromethane (10 mL) was added. The reaction mixture was stirred for 3 h, dried in vacuo, and the solid product washed with hexane to afford a white precipitate which was filtered, dried in vacuo, and analyzed. Yield: 89% (217 mg, 0.445 mmol). ^{1}H NMR ($CDCl_3$): 1.70 (s, 9H, 3(CH_3)), 2.44 (s, 9H, 3(CH_3), 3.68 (s, 6H, 2CH_3 [dmit]), 5.73 (s, 3H, 3CH [Pz]), 6.83 (s, 2H, 2CH [dmit]). ^{13}C{^{1}H} NMR ($CDCl_3$): 13.25 (CH_3), 13.64 (CH_3), 36.08 (CH_3 [dmit]), 104.79 (C-4 [Pz]), 119.33 (2CH [dmit]), 144.60 (C-3 [Pz]), 148.31 (C-5 [Pz]), 157.45 (C=S). IR (cm^{-1}): 502 s, 516 s, 634 s, 656 s, 664 s, 679 s, 699 s, 743 s, 784 s, 813 s, 842 s, 979 s, 1036 s, 1059 s, 1082 s, 1175 b, 1235 s, 1262 s, 1386 b, 1542 s, 1571 s, 1653 s, 1673 s, 1695 s, 1734 s, 2341 s, 2362 s, 2509 s, 2735 s, 2853 b, 3034 s, 3118 s, 3155 s. Mp: 223−227 °C. UV−vis (CH_3CN): 267 nm. Mass spectrum (ESI-MS): *m*/*z* 488.1 [Tp*Cu(dmit)]$^+$, 360.1 [Tp*Cu]$^+$, 318.9 [Cu(dmit)$_2$]$^+$, 190.9 [Cu-dmit]$^+$. Anal. Calcd for $CuC_{20}BH_{30}N_8S$: C, 49.13; N, 22.92; H, 6.20. Found: C, 48.83; N, 22.45; H, 6.18.

Tp*Cu(dmise) (8). Complex **7** was prepared following the procedure for **6** using both methods except that dmise (175 mg, 1 mmol) was used in place of dmit. Single crystals suitable for X-ray analysis were grown by slow vapor diffusion of ether into dichloromethane and methanol solution. Yield: method 1, 59% (316 mg, 0.59 mmol); method 2, 74% (397 mg, 0.74 mmol). ^{1}H NMR ($CDCl_3$): 1.70 (s, 9H, 3(CH_3)), 2.44 (s, 9H, 3(CH_3), 3.75 (s, 6H, 2CH_3 [dmise]), 5.73 (s, 3H, 3CH [Pz]), 6.93 (s, 2H, 2CH [dmise]). ^{13}C{^{1}H} NMR ($CDCl_3$):): 13.25 (CH_3), 13.64 (CH_3), 37.45 (CH_3 [dmise]), 104.79 (C-4 [Pz]), 120.27 (2CH [dmise]), 144.60 (C-3 [Pz]), 148.30 (C-5 [Pz]), 151.63 (C=Se). IR (cm^{-1}): 599 s, 635 s, 655 s, 666 s, 699 s, 723 s, 748 s, 811 w, 839 s, 980 s, 1036 s, 1059 s, 1081 s, 1146 s, 1176 b, 1232 s, 1262 s, 1378 b, 1443 b, 1541 s, 1569 s, 1594 s, 1699 s, 2508 s, 2734 s, 2851 s, 3116 s, 3152 s. Mp: 223−227 °C. UV−vis (CH_3CN): 270 nm. Mass spectrum (ESI-MS): *m*/*z* 536.1 [Tp*Cu(dmise)]$^+$, 414.9 [Cu(dmise)$_2$]$^+$, 360.1 [Tp*Cu]$^+$, 175.9 [dmise]$^+$. Anal. Calcd for $CuC_{20}BH_{30}N_8Se$: C, 46.04; N, 20.45; H, 5.52. Found: C, 45.05; N, 20.89; H, 5.69.

[Tpm*Cu(dmise)][Cl] (9). The dmise ligand (176 mg, 1 mmol) was dissolved in acetonitrile (20 mL) and was cannula transferred to a solution of CuCl (99 mg, 1 mmol) in methanol (20 mL). The reaction mixture was stirred for 3 h at room temperature, and an equimolar amount of Tpm* (298 mg, 1 mmol) was dissolved in acetonitrile and cannula transferred into the reaction mixture and stirred for 18 h. The reaction mixture was pumped down to ∼5 mL, and the target product was precipitated using ether. The precipitate was dried in vacuo to yield a white powder. Yield 52% (297 mg, 0.52 mmol). ^{1}H NMR (CD_2Cl_2): 2.26 (s, 9H, 3CH_3), 2.32 (s, 9H, 3CH_3), 3.75 (s, 6H, 2CH_3 [dmise]), 5.97 (s, 3H, 3CH [Pz]), 6.97 (s, 2H, 2CH [dmise]), 7.87 (s, 1H, CH). ^{13}C{^{1}H} NMR (CD_2Cl_2): 10.70 (CH_3), 13.37

(CH_3), 37.22 (CH_3 [dmise]), 106.99 (C-4 [Pz]), 119.98 (2CH [dmise]), 139.69 (C-3 [Pz]), 149.95 (C-5 [Pz]), 153.22 (C=Se). Mp: 256−258 °C. IR (cm^{-1}): 628 s, 652 s, 700 vs, 705 vs, 738 s, 799 vs, 813 s, 850 vs, 900 vs, 975 vs, 1035 vs, 1098 w, 1150 s, 1240 vs, 1305 s, 1382 s, 1412 s, 1464 s, 1522 w, 1540 w, 1560 vs, 1653 s, 1733 s, 2338 w, 2361 w, 2936 b. UV−vis (CH_3CN): 273 nm. Mass spectrum (ESI-MS): m/z 537.1 $[Tpm*Cu(dmise)]^+$, 402.1 [Tpm*-Cu + MeOH]$^+$, 361.1$[Tpm*Cu]^+$. Molar conductivity: 30.71 S cm^2 mol^{-1}. Anal. Calcd for $C_{21}H_{30}CuN_8SeCl$: C, 44.06; N, 19.57; H, 5.28. Found: C, 43.35; N, 19.43; H, 5.19.

[Tpm*Cu(dmit)][Cl] (10). Complex **10** was prepared following the procedure for **9** except that dmit (129 mg, 1 mmol) was used in place of dmise. Yield: 60% (315 mg, 0.60 mmol). ^1H NMR (CD_2Cl_2): 2.16 (s, 9H, $3CH_3$), 2.55 (s, 9H, $3CH_3$), 3.73 (s, 6H, $2CH_3$ [dmit]), 6.06 (s, 3H, 3CH [Pz]), 6.86 (s, 2H, 2CH [dmit]), 7.912 (s, 1H, CH). $^{13}C\{^1H\}$ NMR (CD_2Cl_2): 9.43 (CH_3), 12.04 (CH_3), 34.63 (CH_3 [dmit]), 68.59 (CH), 106.40 (C-4 [Pz]), 119.42 (CH [dmit]), 140.38 (C-3 [Pz]), 150.61 (C-5 [Pz]), 156.54 (C=S). IR (cm^{-1}): 630 s, 664 s, 670 s, 699 s, 706 s, 734 s, 749 s, 763 s, 817 s, 849 vs, 898 s, 977 s, 1035 s, 1087 s, 1181 b, 1240 s, 1306 s, 1387 b, 1465 b, 1521 s, 1567 s, 1623 b, 1653 b, 2915 b, 3074 b, 3105 b. Mp: 275−277 °C. UV−vis (CH_3CN): 273 nm. Mass spectrum (ESI-MS): m/z 489.1 $[Tpm*Cu(dmit)]^+$, 402.1 [Tpm*-Cu + MeOH]$^+$, 361.1 $[Tpm*Cu]^+$. Molar conductivity: 25.10 S cm^2 mol^{-1}. Anal. Calcd for $C_{21}H_{30}CuN_8SCl$: C, 47.91; N, 21.29; H, 5.71. Found: C, 47.65; N, 21.05; H, 5.69.

[Tpm$^{i\mathrm{Pr}}$Cu(dmit)][Cl] (11). Complex **11** was prepared following the procedure for **9** except that dmit (129 mg, 1 mmol) and Tpm$^{i\mathrm{Pr}}$ (466 mg, 1 mmol) were used in place of dmise and Tpm*, respectively. Yield: 62% (430 mg, 0.62 mmol). ^1H NMR ($CDCl_3$): 1.22 (d, J_{HH} = 6 Hz, 36H, $6(CH_3)_2$), 3.11 (sept, J_{HH} = 8.25 Hz, 3H, 3CH), 3.19 (br, 3H, 3CH), 3.70 (s, 6H, $2CH_3$ [dmit]), 5.94 (s, 3H, 3CH [Pz]), 6.82 (s, 2H, 2CH [dmit]), 8.04(s, 1H, CH). $^{13}C\{^1H\}$ NMR ($CDCl_3$): 22.64 ($CH(CH_3)_2$), 23.13 ($CH(CH_3)_2$), 25.88 ($CH(CH_3)_2$), 27.73 ($CH(CH_3)_2$), 35.64 (CH_3 [dmit]), 63.43 (HC), 99.96 (4-C (Pz)), 118.58 ($2CH_2$ [dmit]), 150.76 (3-C (Pz)), 159.5 (C=S), 160.09 (5-C (Pz)). IR (cm^{-1}): 670 vs, 691 s,722 vs, 747 vs, 763 vs, 797 vs, 806 s, 826 s, 861 s, 879 s, 903 s, 927 s, 961 s, 999 w, 1016 s, 1057 s, 1071 s, 1109 s, 1177 s, 1243 s, 1270 s, 1291 s, 1309 s, 1364 s,1380 s, 1465 w, 1552 s, 1571 s, 1621 s, 1656 b, 1729 s, 2722 b, 3038 b, 3079 s, 3104 s, 3148 s, 3196 b. Mp: 223−227 °C. UV−vis (CH_3CN): 260 nm. Mass spectrum (ESI-MS): m/z 657.2 $[Tpm^{i\mathrm{Pr}}Cu(dmit)]^+$, 529.3 $[Tpm^{i\mathrm{Pr}}Cu]^+$, 319.0 $[Cu(dmit)_2]^+$, 232.0 [Cu-dmit + MeOH]$^+$, 191.0 [dmit-Cu]$^+$. Molar conductivity: 24.54 S cm^2 mol^{-1}. Anal. Calcd for $C_{33}H_{54}CuN_8SCl$: C, 57.14; N, 16.16; H, 7.79. Found: C, 56.40; N, 15.69; H, 7.88.

[Tpm$^{i\mathrm{Pr}}$Cu(dmise)][Cl] (12). Complex **12** was prepared following the above procedure for **9** except that Tpm$^{i\mathrm{Pr}}$ (466 mg, 1 mmol) was used in place of Tpm*. Yield: 42% (311 mg, 0.42 mmol). ^1H NMR ($CDCl_3$): 1.22 (d, J_{HH} = 6 Hz, 36H, $6(CH_3)_2$), 3.10 (sept, J_{HH} = 6 Hz, 3H, 3CH), 3.19 (sept, J_{HH} = 6 Hz, 3H, 3CH), 3.79 (s, 6H, $2CH_3$ [dmise]), 5.94 (s, 3H, 3CH [Pz]), 6.98 (s, 2H, 2CH [dmise]), 8.04 (s, 1H, CH). $^{13}C\{^1H\}$ NMR ($CDCl_3$): 22.66 ($CH(CH_3)_2$), 23.13 ($CH(CH_3)_2$), 25.93 ($CH(CH_3)_2$), 27.72 ($CH(CH_3)_2$), 37.56 (CH_3 [dmise]), 71.1 (HC), 99.92 (4-CH [Pz]), 120.54 (2CH [dmise]), 150.81 (3-CH [Pz]), 152.03 (C=Se), 160.25 (5-CH [Pz]). IR (cm^{-1}): 668 vs, 722 vs, 740 vs, 752 vs, 797 vs, 806 s, 825 s, 860 s, 879 s, 903 s, 927 s, 1004 s, 1015 s, 1056 s, 1072 s, 1109 s, 1151 s, 1180 vs, 1234 s, 1270 vs, 1290 s, 1308 s, 1380 s, 1464 b, 1552 s, 1565 s, 1595 b, 1656 b, 2125 b, 3093 b, 3146 s. Mp: 234−236 °C. UV−vis (CH_3CN): 205, 268 nm. Mass-spectrum (ESI-MS): m/z 705.2 $[Tpm^{i\mathrm{Pr}}Cu(dmise)]^+$, 570.3 [Tpm$^{i\mathrm{Pr}}$Cu + MeOH]$^+$, 529.2 $[Tpm^{i\mathrm{Pr}}Cu]^+$, 414.9 $[Cu(dmise)_2]^+$. Molar conductivities: 23.29 S cm^2 mol^{-1}. Anal. Calcd for $C_{33}H_{54}CuN_8SeCl$: C, 53.51; N, 15.14; H, 7.30. Found: C, 52.89; N, 15.21; H, 7.25.

X-ray Data Collection and Structural Determination. Single crystals grown from vapor diffusion were mounted on a glass filament with silicon grease and immediately cooled to 168 ± 2 K in a cold nitrogen gas stream. The crystals were grown by vapor diffusion of diethyl ether into an acetonitrile solution for [Tpm*Cu(dmise)][BF_4] (**1**) and [Tpm*Cu(dmit)][BF_4] (**2**); diethyl ether into a methanol solution for [TpmCu(dmise)][BF_4] (**3**) and [TpmCu(dmit)][BF_4] (**4**); diethyl ether into dichloromethane solution for [Tpm$^{i\mathrm{Pr}}$Cu(dmise)][BF_4] (**6**); and diethyl ether into a dichloromethane/methanol solution for Tp*Cu(dmit) (**7**) and Tp*Cu(dmise) (**8**). Intensity data were collected using a Rigaku Mercury CCD detector and an AFC8S diffractometer. The space groups $P2_1/c$ for **1**, **2**, and **3**; $P2_12_12_1$ for **4**; $C2/c$ for **6** and $P2_1/m$ for **7** and **8** were determined from the observed systematic absences. Data reduction including the application of Lorentz and polarization (Lp) effects and absorption corrections used the CrystalClear program.[51] The structures were solved by direct methods and subsequent Fourier difference techniques, and refined anisotropically, by full-matrix least-squares, on F^2 using SHELXTL 6.10.[52] The quantity minimized by the least-squares program was $\sum w(F_o^2 - F_c^2)^2$ where $w = \{[\sigma^2(F_o^2)] + (0.0585P)^2 + 1.89P]\}$ for **1**, $w = \{[\sigma^2(F_o^2)]\} + (0.0843P)^2 + 1.58P]\}$ for **2**, $w = \{[\sigma^2(F_o^2)] + (0.0298P)^2 + 46.69P]\}$ for **3**, $w = \{[\sigma^2(F_o^2)] + (0.0469P)^2 + 0.34P]\}$ for **4**, $w = \{[\sigma^2(F_o^2)] + (0.0993P)^2 + 4.78P]\}$ for **6**, $w = \{[\sigma^2(F_o^2)] + (0.0619P)^2 + 0.93P]\}$ for **7**, $w = \{[\sigma^2(F_o^2)] + (0.537P)^2 + 1.39P]\}$ for **8**, and $P = (F_o^2) + 2F_c^2)/3]$. In the final cycle of least squares, independent anisotropic displacement factors were refined for the non-hydrogen atoms, and the methyl hydrogen atoms were fixed in idealized positions with C−H = 0.96 Å. Their isotropic displacement parameters were set equal to 1.5 times U_{eq} of the attached carbon atom.

For complex **1**, the largest peak in the final Fourier difference map (0.81 e Å^{-3}) was located 0.92 Å from F2, and the lowest peak (−0.68 e Å^{-3}) was located at a distance of 0.81 Å from Se. The largest peak for complex **2** in the final Fourier difference map (1.014 e Å^{-3}) was located 0.02 Å from Cu, and the lowest peak (−0.676 e Å^{-3}) was located at a distance of 0.76 Å from Cu. The largest peak for complex **3** in the final Fourier difference map (1.635 e Å^{-3}) was located 0.29 Å from H3AA, and the lowest peak (−0.740 e Å^{-3}) was located at a distance of 0.80 Å from Se1A. The largest peak for **4** in the final Fourier difference map (0.77 e Å^{-3}) was located 1.59 Å from H11A, and the lowest peak (−0.41 e Å^{-3}) was located at a distance of 0.80 Å from Cu. The largest peak for **6** in the final Fourier difference map (0.94 e Å^{-3}) was located 0.04 Å from Se1, and the lowest peak (−0.60 e Å^{-3}) was located at a distance of 0.89 Å from Se1. The largest peak for **7** in the final Fourier difference map (0.583 e Å^{-3}) was located 0.92 Å from H20B, and the lowest peak (−0.628 e Å^{-3}) was located at a distance of 0.11 Å from H20A. The largest peak for **8** in the final Fourier difference map (0.71 e Å^{-3}) was located 2.44 Å from H13B and the lowest peak (−0.51 e Å^{-3}) was located 0.81 Å from Se1. Final refinement parameters for the structures of **1**, **2**, **3**, **4**, **6**, and **7** are given in Tables 1 and 2, and selected bond angles and distances are summarized in Tables 4 and 5. The crystal structure diagram and selected bond angles and distances for Tp*Cu(dmise) (**8**) are reported in Figure 3 and Table S2 (Supporting Information).

Results and Discussion

Synthesis of Cu(I) Selone and Thione Complexes. The target copper(I) complexes with the BF_4^- counterion were synthesized using two different routes. Method 1 involves a two-step, one-pot procedure via the treatment of equimolar amounts of [$Cu(NCCH_3)_4$][BF_4] and *N,N′*-dimethylimidazole selone (dmise) or *N,N′*-dimethylimidazole thione (dmit) in acetonitrile followed by cannula

(51) *CrystalClear*; Rigaku/MSC: The Woodlands, TX, 1999.
(52) Sheldrick, G. M. *SHELXTL, Structure Determination Software Programs*, Version 6.1; Bruker Analytical X-ray Systems Inc.: Madison, WI, 2000.

Table 1. Summary of Crystallographic Data for Complexes **1**, **2**, and **3**

	1	**2**	**3**
chemical formula	$C_{21}H_{30}BCuF_4N_8Se$	$C_{21}H_{30}BCuF_4N_8S$	$C_{15}H_{18}BCuF_4N_8Se$
F.W. (g/mol)	623.84	576.94	539.69
space group	$P2_1/c$	$P2_1/c$	$P2_1/c$
crystal system	monoclinic	monoclinic	monoclinic
a, Å	12.199(2)	12.248(2)	10.176(2)
b, Å	16.322(3)	16.233(3)	17.734(3)
c, Å	13.043(3)	12.914(3)	22.586(4)
α, deg	90	90	90
β, deg	93.54(3)	93.41(3)	96.47(3)
γ, deg	90	90	90
V, Å^3	2592.2(9)	2563.2(9)	4049.9(13)
Z	4	4	8
D_{cal}, Mg/m^3	1.598	1.495	1.770
indices (min)	[−15, −20, −16]	[−15, −20, −16]	[−12, −21, −24]
indices (max)	[12, 20, 15]	[13, 19, 16]	[11, 21, 26]
parameters	333	333	546
F(000)	1264	1192	2144
μ, mm^{-1}	2.302	0.990	2.932
2θ range, deg	2.50−26.71	3.01- 26.73	2.96−25.05
collected reflections	21217	22159	30276
unique reflections	5472	5406	7119
final R (obs. data)[a], R_1	0.0435	0.0508	0.0692
wR_2	0.1101	0.1349	0.1713
final R (all data), R_1	0.0508	0.0557	0.0741
wR_2	0.1163	0.1426	0.1732
goodness of fit (S)	1.110	1.098	1.180
largest diff. peak	0.808	1.014	1.490
largest diff. hole	−0.682	−0.676	−0.619

[a] $R_1 = \sum||F_o| - |F_c||/\sum|F_o|$; $wR_2 = \{\sum w(F_o^2 - F_c^2)^2\}^{1/2}$.

Table 2. Summary of Crystallographic Data for Complexes **4**, **6**, **7**, and **8**

	4	**6**	**7**	**8**
chemical formula	$C_{15}H_{18}BCuF_4N_8S$	$C_{33}H_{54}BCuF_4N_8Se$	$C_{20}BH_{30}CuN_8S$	$C_{20}BH_{30}CuN_8Se$
F.W. (g/mol)	492.78	792.15	488.93	535.83
space group	$P2(1)2(1)2(1)$	$C2/c$	$P2_1/m$	$P21/m$
crystal system	orthorhombic	monoclinic	monoclinic	monoclinic
a, Å	9.7241(19)	23.822(5)	8.2925(17)	8.3319(17)
b, Å	11.335(2)	16.733(3)	11.808(2)	11.771(2)
c, Å	18.262(4)	19.931(4)	11.934(4)	12.082(2)
α, deg	90	90	90	90
β, deg	90	100.04(3)	91.32(3)	92.09(3)
γ, deg	90	90	90	90
V, Å^3	2012.9(7)	7823(3)	1168.3(4)	1184.2(4)
Z	4	8	2	2
D_{cal}, Mg/m^3	1.626	1.345	1.390	1.503
indices (min)	[−8, −14, −23]	[−29, −20, −21]	[−10, −14, −14]	[−9, −14, −15]
indices (max)	[12, 14, 23]	[28, 20, 24]	[9, 14, 14]	[10, 14, 11]
parameters	274	447	160	160
F(000)	1000	3296	512	548
μ, mm^{-1}	1.245	1.541	1.048	2.483
2θ range, deg	2.76−26.72	2.43−26.32	3.02−26.74	3.02−26.29
collected reflections	16710	38614	11607	9538
unique reflections	4255	7938	2586	2494
final R (obs. data)[a], R_1	0.0354	0.0628	0.0394	0.0383
wR_2	0.0845	0.1619	0.1041	0.0953
final R (all data), R_1	0.0388	0.1023	0.0413	0.0465
wR_2	0.0871	0.1969	0.1073	0.1021
goodness of fit (S)	1.139	1.050	1.102	1.059
largest diff. peak	0.766	0.941	0.583	0.712
largest diff. hole	−0.412	−0.598	−0.628	−0.513

[a] $R_1 = \sum||F_o| - |F_c||/\sum|F_o|$; $wR_2 = \{\sum w(F_o^2 - F_c^2)^2\}^{1/2}$.

addition of the desired tripodal ligand in acetonitrile. Method 2 involves treating $[Tpm^RCu(NCCH_3)][BF_4]$ with one molar equivalent of dmise or dmit in dichloromethane (Scheme 1). Compared to method 1, method 2 generally results in slightly higher yields with shorter reaction times. Copper complexes with the chloride counterion were synthesized by reaction of equimolar amounts of CuCl and the chalcogenone in a mixed solvent system of methanol and acetonitrile, followed by cannula addition of the tripodal ligand in acetonitrile (Scheme 1).

The neutral copper complexes were synthesized by combining CuCl and dmise/dmit in methanol and acetonitrile, respectively, followed by cannula addition of tris(3,5-dimethylpyrazolyl)borate (Tp*) in acetonitrile (Scheme 1).

Scheme 1

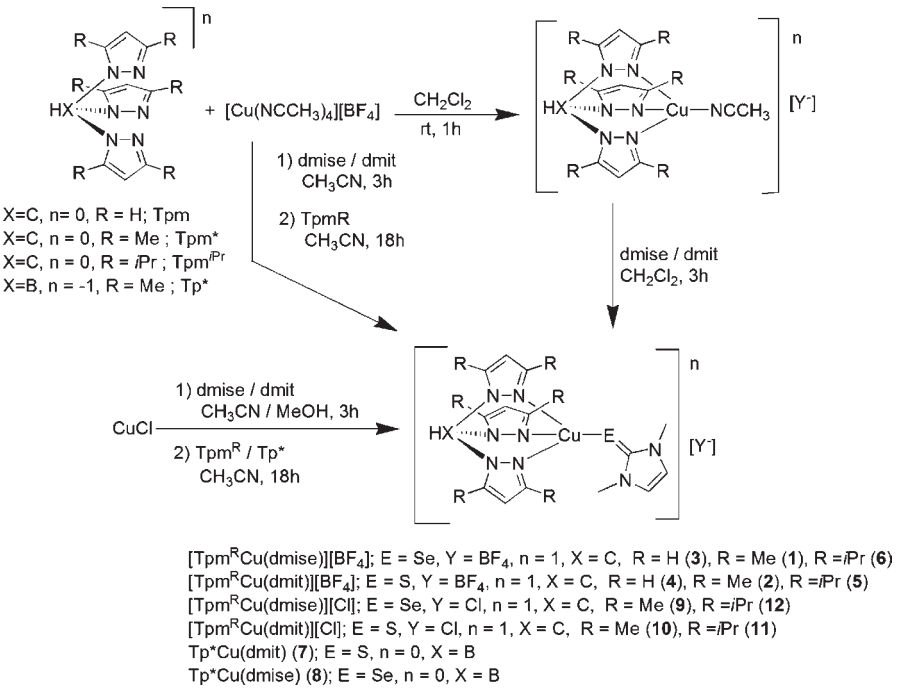

These neutral complexes can also be synthesized by reaction of Tp*Cu($NCCH_3$) with molar equivalent of dmit or dmise in dichloromethane (Scheme 1). All of the target metal complexes are fairly stable to air for about 5−10 h as solids but are easily oxidized from Cu^+ to Cu^{2+} in solution.

NMR Spectroscopy of Copper Thione and Selone Complexes. In the ^{1}H NMR spectra of [Tpm^{R}Cu(L)][X] (R = H; Tpm, R = Me; Tpm*, R = *i*Pr; Tpm^{iPr}; L = $NCCH_3$, dmise, or dmit; X = BF_4^- or Cl^-), the apical CH proton resonance of the tris(pyrazolyl)methane ligand bound to copper is shifted upfield by δ 0.1 to 0.5 from its position in the free ligand. This same upfield shift was observed by Fujisawa and co-workers for the [Tpm^{iPr}Cu($NCCH_3$)]$^+$ complex.[42] All other proton signals of both the tripodal ligand (Tpm^R) and the chalcogenone (dmise and dmit) are shifted downfield upon Cu^+ complexation. This downfield shift of the ligand resonance upon copper coordination is a result of increased deshielding effects on the protons upon metal binding. For copper complexes with tris(pyrazolyl)borate ligands, the resonance for the BH proton is not observed, as is common.[42]

^{1}H and ^{13}C{^{1}H} NMR spectroscopy data for the complexed and uncomplexed selone and thione ligands are given in Table 3 (ligand numbering scheme in Figure 1A). A substantial shift of the C-2 resonance of the dmise and dmit ligands is observed upon complexation to copper. Shifts of δ 3 to 8 for both the C=Se and the C=S carbons are also observed upon copper binding, attributed to the shift of the electron density from the selenocarbonyl or thiocarbonyl group to the neighboring N−C bond. This electron density shift reduces the double bond character of the C=Se or C=S bond while increasing that of the C−N single bond, resulting in an upfield shift for the C-2 resonance.[33,53−55] This upfield shift is characteristic of selone or thione bound to copper via the selenium and sulfur atoms. The increased electron density of the C−N bond upon copper complexation results in a minor increases in deshielding effects on C-4 and C-5, as supported by observed downfield shifts of the C-4 and C-5 resonances. In the ^{1}H and ^{13}C{^{1}H} NMR spectra, H-4/5 and are shifted downfield and C-2 resonances are shifted upfield for the selone copper complexes (δ 6.93−7.18 and δ 120.3−122.2, respectively) and thione copper complexes (δ 6.82−7.04 and δ 118.6−119.9, respectively) relative to the free selone (δ 6.77 and δ 119.7) and thione (δ 6.64 and δ 117.6) compounds (Table 3). These NMR shifts upon selone and thione complexation are consistent with copper binding stabilizing the resonance form that

Table 3. ^{13}C{^{1}H} and ^{1}H NMR Chemical Shifts of Selone and Thione Ligands before and after Copper Complexation

	^{13}C{^{1}H} shift (δ)		^{1}H shift (δ)	
ligand or Cu(I) complex	C-2	C-4/5	CH_3	H-4/5
Dmise	155.57	119.71	3.53	6.77
[TpmCu(dmise)][BF_4] (**3**)	148.90	122.24	3.73	7.15
[Tpm*Cu(dmise)][BF_4] (**1**)	147.61	121.60	3.88	7.17
[Tpm^{iPr}Cu(dmise)][BF_4] (**6**)	148.12	121.47	3.85	7.18
[Tpm*Cu(dmise)][Cl] (**9**)	153.22	119.98	3.75	6.97
[Tpm^{iPr}Cu(dmise)][Cl] (**12**)	152.03	120.54	3.79	6.98
Tp*Cu(dmise) (**8**)	151.63	120.27	3.75	6.93
dmit	162.42	117.60	3.53	6.64
[TpmCu(dmit)][BF_4] (**4**)	154.66	119.90	3.82	7.04
[Tpm*Cu(dmit)][BF_4] (**2**)	155.96	119.70	3.80	7.00
[Tpm^{iPr}Cu(dmit)][BF_4] (**5**)	155.49	119.80	3.77	7.03
[Tpm*Cu(dmit)][Cl] (**10**)	156.54	119.42	3.73	6.86
[Tpm^{iPr}Cu(dmit)][Cl] (**11**)	159.52	118.58	3.70	6.82
Tp*Cu(dmit) (**7**)	157.45	119.33	3.68	6.83

(53) Beheshti, A.; Clegg, W.; Nobakht, V.; Mehr, M. P.; Russo, L. *Dalton Trans.* **2008**, 6641–6646.

(54) Popovic, Z.; Pavlovic, G.; Matkovic-Calogovic, D.; Soldin, Z.; Rajic, M.; Vikic-Topic, D.; Kovacek, D. *Inorg. Chim. Acta* **2000**, *306*, 142–152.

(55) Bierbach, U.; Hambley, T. W.; Farrell, N. *Inorg. Chem.* **1998**, *37*, 708–716.

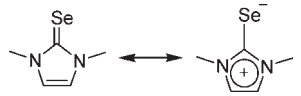

Figure 2. Resonance structures for the selone ligand.

places the positive charge into the heterocyclic ring (Figure 2).

Notably, the copper complexes with Cl^- counterions have smaller downfield shift on the methyl and olefinic protons and smaller upfield C-2 resonance shifts of the heterocyclic chalcogenones relative to analogous complexes with BF_4^- counterions. Because Cl^- is significantly more coordinating than BF_4^-, the Cl^- counterion may compete slightly with the selone ligand for binding to labile Cu^+.[56,57] The presence of mononuclear copper complexes with dmise and dmit ligands can be clearly seen from their ESI-mass spectra. The fragmentation patterns found for all the complexes are consistent with their calculated isotopic distributions.

Molar conductivities in DMF solution of the neutral complexes $Tpm^{iPr}CuCl$ and Tpm*CuCl are low (18.4 and 19.2 S cm^2 mol^{-1}, respectively), indicating chloride coordination. In contrast, molar conductivities of the cationic complexes **1**, **2**, **5**, and **6** with non-coordinating BF_4^- anions are significantly higher (89.7−118.4 S cm^2 mol^{-1}), indicating 1:1 ionic complexes. Conductivities of compounds with Cl^- anions (**9**, **10**, **11**, and **12**) range from 23.3 to 30.7 S cm^2 mol^{-1}, indicating that the Cl^- anions compete with thione and selone for copper binding. The ^1H NMR resonances for the H-4/5 protons of the copper chloride complexes **9**, **10**, **11**, and **12** (δ 6.82−6.98) are closer to the unbound ligands compared to complexes **1**, **2**, **5**, and **6** with non-coordinating BF_4^- counterions (δ 7.00−7.18), corroborating the conductivity measurements.

IR Spectroscopy. The acetonitrile copper complexes used as starting materials, $[Tpm^*Cu(NCCH_3)][BF_4]$ and $[Tpm^{iPr}Cu(NCCH_3)][BF_4]$ have N≡C stretching frequencies of 2272 and 2275 cm^{-1}, respectively, comparable to literature reports.[58] The N≡C stretches in these copper acetonitrile complexes are shifted to higher wavenumbers relative to free acetonitrile (2250 cm^{-1}), indicating an increased N≡C bond strength because of donor bond formation upon Cu^+ complexation.[59] The IR spectrum of dmit shows a C=S stretching vibration at ∼1181 cm^{-1}, whereas dmise has a C=Se stretching vibration at ∼1148 cm^{-1}, consistent with previous reports for dmit, 1-mesitylimidazole selone, mbit = 1,1′-methylenebis(1,3-dihydro-3-methyl-2*H*-imidazole-2-thione), and mbis = 1,1′-methylene-bis(1,3-dihydro-3-methyl-2*H*-imidazole-2-selone).[60−62] Upon copper-dmit binding in complexes **2**, **4**, **5**, and **7** this C=S stretch shifts to lower energy, 1172−1178 cm^{-1}, indicative of weak backbonding to the thione ligand. Coordination of dmise to copper in Tpm^R complexes **1**, **3**, and **6** results in a slight shift of C=Se stretch to higher energy, 1150−1151 cm^{-1}, indicating that backbonding interactions with this ligand are not significant. In contrast, the IR spectrum of Tp*Cu(dmise) (**8**) shows a slight shift to lower energy region for C=Se stretch (1145 cm^{-1}) upon coordination of dmise to copper.

Table 4. Selected Bond Lengths (Å) and Angles (deg) for Complexes **1**, **3**, and **6**

	1	**3**	**6**
Cu(1)−N(3)	2.126(2)	2.188(6)	2.058(4)
Cu(1)−N(4)	2.063(3)	2.111(6)	2.095(4)
Cu(1)−N(5)	2.089(2)	2.053(6)	2.189(4)
Cu(1)−Se(1)	2.2981(6)	2.2941(13)	2.3126(8)
Se(1)−C(1)	1.868(3)	1.880(7)	1.858(5)
N(4)−Cu(1)−N(5)	88.66(10)	88.8(2)	84.62(16)
N(4)−Cu(1)−N(3)	87.66(10)	86.6(2)	88.44(16)
N(5)−Cu(1)−N(3)	85.67(9)	86.1(2)	85.43(16)
N(3)−Cu(1)−Se(1)	125.46(7)	122.35(17)	130.52(11)
N(4)−Cu(1)−Se(1)	132.37(7)	132.94(17)	124.40(11)
N(5)−Cu(1)−Se(1)	123.04(7)	125.80(17)	128.71(10)
C(1)−Se(1)−Cu(1)	108.24(10)	100.4(2)	104.62(13)

Table 5. Selected Bond Lengths (Å) and Angles (deg) for Complexes **2**, **4**, and **7**

	2	**4**	**7**
Cu−N(3)	2.095(2)	2.128(2)	2.1248(16)
Cu−N(3A)			2.1248(16)
Cu−N(4)	2.077(2)	2.121(2)	2.039(2)
Cu−N(5)	2.1334(19)	2.117(2)	
Cu−S	2.191(8)	2.202(7)	2.219(9)
S−C(1)	1.709(3)	1.711(3)	1.708(3)
N(3)−Cu−N(4)	88.49(8)	88.73(9)	92.09(7)
N(3A)−Cu−N(5)			92.09(7)
N(3)−Cu−N(5)	85.23(8)	87.82(9)	
N(4)−Cu−N(5)	87.40(8)	85.5(10)	87.23(9)
N(3)−Cu-S	125.20(6)	111.8(6)	119.14(5)
N(3A)−Cu-S			119.14(5)
N(4)−Cu-S	130.45(6)	133.15	134.84(7)
N(5)−Cu-S	126.07(6)	134.51	
C(1)−S−Cu	111.30(9)	106.8(9)	105.62(10)

Structural Analysis of Copper Selone and Thione Complexes. Single crystal X-ray diffraction data were collected for $[Tpm^*Cu(dmise)][BF_4]$ (**1**), $[Tpm^*Cu(dmit)][BF_4]$ (**2**), $[TpmCu(dmit)][BF_4]$ (**4**), $[Tpm^{iPr}Cu(dmise)][BF_4]$ (**6**), Tp*Cu(dmit) (**7**) and Tp*Cu(dmise) (**8**), which crystallized as colorless prisms, and for $[TpmCu(dmise)][BF_4]$ (**3**), which crystallized as colorless rods. Their structural parameters are summarized in Tables 4, 5, and Supporting Information, Table S2, and their structures are shown in Figures 3, 4, and 5. All the Cu^+ centers adopt distorted tetrahedral coordination geometry, bound to three nitrogen atoms from the tridentate ligand in a κ^3-fashion, and terminally bound to the heterocyclic chalcogenones. The distorted tetrahedral geometries can be seen in the N−Cu−N angles, ranging from 84.6 to 92.1° and arise from pinning back of Tpm^R and KTp* nitrogen atoms because of the small bite angles of these ligands.[46]

The crystal structure of $[TpmCu(dmise)][BF_4]$ (**3**) is composed of two crystallographically independent molecules in the same unit cell (Figure 3 and Supporting Information, Figure S1; Table 4 and Supporting Information,

(56) Takeda, N.; Tanaka, Y.; Sakakibara, F.; Unno, M. *Bull. Chem. Soc. Jpn.* **2010**, *83*, 157–164.
(57) Parker, L. L.; Lacy, S. M.; Farrugia, L. J.; Evans, C.; Robins, D. J.; O'Hare, C. C.; Hartley, J. A.; Jaffar, M.; Stratford, I. J. *J. Med. Chem.* **2004**, *47*, 5683–5689.
(58) Balili, M. N. C.; Pintauer, T. *Acta Crystallogr.* **2007**, *E63*, M988–M990.
(59) Swanson, B.; Shriver, D. F.; Ibers, J. A. *Inorg. Chem.* **1969**, *8*, 2182–2189.
(60) Williams, D. J.; Ly, T. A.; Mudge, J. W.; Vanderveer, D.; Jones, R. L. *Inorg. Chim. Acta* **1994**, *218*, 133–138.
(61) Landry, V. K.; Minoura, M.; Pang, K. L.; Buccella, D.; Kelly, B. V.; Parkin, G. *J. Am. Chem. Soc.* **2006**, *128*, 12490–12497.
(62) Jia, W. G.; Huang, Y. B.; Lin, Y. J.; Wang, G. L.; Jin, G. X. *Eur. J. Inorg. Chem.* **2008**, 4063–4073.

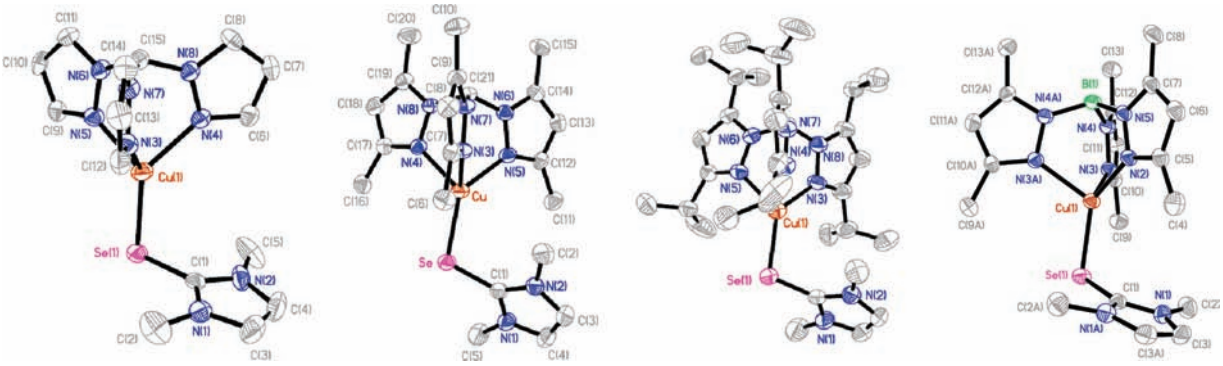

Figure 3. Crystal structure diagrams with 50% probability density ellipsoids of (from left) [TpmCu(dmise)][BF_4] (**3**), [Tpm*Cu(dmise)][BF_4] (**1**), [Tpm$^{i\mathrm{Pr}}$Cu(dmise)][BF_4] (**6**), and Tp*Cu(dmise) (**8**). Hydrogen atoms and counterions are omitted for clarity.

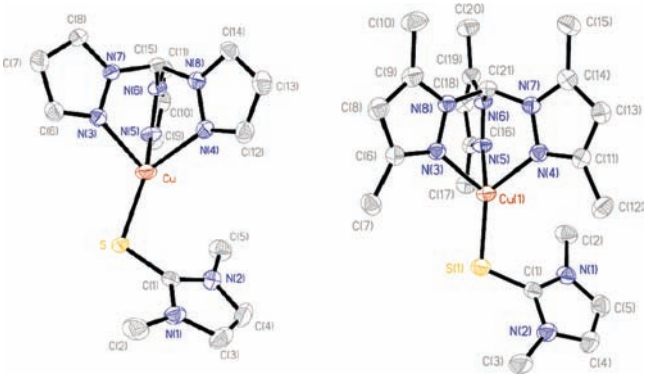

Figure 4. Crystal structure diagrams (50% probability density ellipsoids) of [TpmCu(dmit)][BF_4] (**2**; left) and [Tpm*Cu(dmit)][BF_4] (**4**; right). Hydrogen atoms and counterions are omitted for clarity.

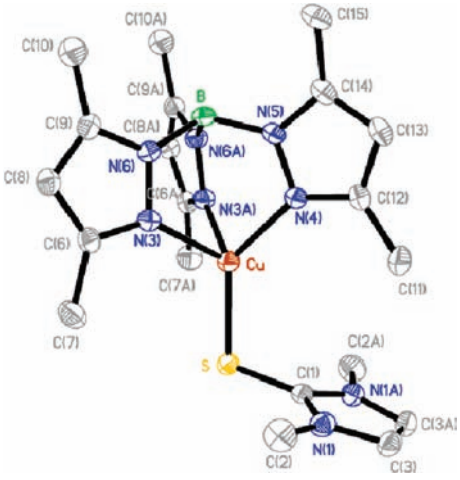

Figure 5. Crystal structure diagram with 50% probability density ellipsoids of Tp*Cu(dmit) (**7**). Hydrogen atoms omitted for clarity.

Table S1). Each copper atom adopts a distorted tetrahedral coordination environment with average Cu−N distances of 2.12 Å for Cu(1)−N and 2.13 Å for Cu(1A)−N(A). Mean N−Cu−N angles are 87.2° for N−Cu(1)−N and 86.9° for N(A)−Cu(1A)−N(A), respectively. The Cu−Se bond lengths and Cu−Se−C bond angles are the major differences between the molecular geometry of these independent molecules, with the Cu(1A) molecule exhibiting a bond length of 2.314 Å and an angle of 110.3° and the Cu(1) molecule a slightly shorter bond length of 2.294 Å and a much smaller angle of 100.4°.

Structures of the Tpm, Tpm*, Tpm$^{i\mathrm{Pr}}$, and Tp* copper selone complexes (**1**, **3**, **6**, and **8**; (Figure 3; Table 4) are very similar despite the differences in steric bulk of their tris(pyrazolyl)methane ligands and overall charge of the ligands. In **1**, **3**, **6**, and **8** the dmise ligand is bound to the copper center with an average angle of 105.2° because of the presence of the lone pairs on the selenium atom. The Cu−Se bond lengths for **1** (2.30 Å), **3** (2.29 Å and 2.31 Å), and **6** (2.31 Å) are comparable, whereas the Cu−Se bond in **8** (2.33 Å) is slightly longer. The Cu−Se bond distances in **1**, **3**, **6**, and **8** are comparable to the Cu−Se bond distance of 2.30 Å in the Cu^{III}-bis-diselenolene complex reported by Ribas et al.,[63] but shorter than most reported copper−selenium complexes such as the selone [Cu(1,10-phen)$_2$($C_5H_{10}N_2Se$)][2ClO_4] (2.49 Å);[37] the selenolate [CuSe(2,4,6-iPr$_3$$C_6H_2$)]$_2$[bipy]$_2$ (2.45 Å);[64] the selenoether [Cu(*o*-C_6H_4(SeMe)$_2$)$_2$]-[PF_6] (2.42 Å);[65] and the selenium macrocycle [Cu($C_{11}H_{14}Se_2$)$_2$][BF_4] (avg. 2.41 Å).[66] Short Cu−Se bond distances for **1**, **3**, **6**, and **8** imply stronger donor interactions between the soft selenium ligand and the soft copper metal ion, but only a limited number of non-bridging copper selone complexes are available for structural comparison. Short interactions of 3.59 Å between selenium atoms are found within the unit cell of [Tpm$^{i\mathrm{Pr}}$Cu(dmise)][BF_4] (**6**), and these interactions are shorter than the sum of Se−Se van der Waals radii (3.80 Å; Supporting Information, Figure S2.)

The copper(I) thione complexes **2**, **4**, and **7** are tetrahedrally coordinated via the three nitrogen atoms of the Tpm* (**2**), Tpm (**4**), or Tp* (**7**) ligands and the sulfur atom of dmit (Figures 4 and 5; Table 5). The average Cu−N distance of 2.10 Å in complex **7** is similar to complex **2**, but shorter compared to Cu−N distances of 2.12 Å in complex **4**. The thione ligand is bound to the copper ion at almost identical C−S−Cu angles in complexes **4** (106.9°) and **7** (105.6°), but the angle increases to 111.3° in complex **2**. Complex **7** has a Cu−S bond distance of 2.22 Å, slightly longer than the observed bond length of 2.19 Å for complex **2** and 2.20 Å for complex **4**. The Cu−S

(63) Ribas, X.; Dias, J.; Morgado, J.; Wurst, K.; Almeida, M.; Veciana, J.; Rovira, C. *CrystEngComm*. **2002**, *4*, 564–567.
(64) Ohlmann, C. M.; Marchland, C. M.; Schonberg, H. *Z. Anorg. Allg. Chem*. **1996**, *622*, 1349–1357.
(65) Black, J. R.; Champness, N. R.; Levason, W.; Reid, G. *Inorg. Chem*. **1996**, *35*, 1820–1824.
(66) Booth, D. G.; Levason, W.; Quirk, J. J.; Reid, G.; Smith, S. M. *J. Chem. Soc., Dalton Trans*. **1997**, 3493–3500.

bond lengths of complexes **2**, **4**, and **7** are shorter than previously reported copper thione complexes such as $[Cu(PPh_3)_2(bzimH_2)Cl]$ (2.38 Å),[34] $[Cu(diditme)_2Cl]$ (2.23 Å),[67] $[CuCl(1\kappa S\text{-imzSH})(PPh_3)_2]$ (2.36 Å),[17] and $[Cu(HB(3,5\text{-}i\text{PrPz})_3(SMeIm)]$ (2.45 Å);[68] however, the Cu−S bond lengths of complexes **2**, **4**, and **7** are longer than those of copper thiolate complexes such as $[Cu(SC_6F_5)(HB(3,5\text{-}i\text{PrPz})_3)]$ (2.18 Å),[41] and $[Cu(SCPh_3)(HB(3,5\text{-}i\text{PrPz})_3)]$ (2.12 Å).[41]

Changing the alkyl substituents on the 3 and 5 positions of the pyrazole ring has minor effects on Cu−Se/S bond distances and Cu−Se/S-C(1) bond angles. In addition, the overall charge of the tris(pyrazolyl) ligand has very little effect on the structure of copper thione complexes. Complex **7** with the negatively charged Tp* ligand has slightly larger N−Cu−N angles (avg. 90.5°) compared to the neutral Tpm and Tpm* ligands (avg. 87.2°). The Cu−S bond distance of 2.19 Å in $[Tpm^*Cu(dmit)][BF_4]$ (**2**) is slightly shorter relative to 2.22 Å in the neutral complex Tp*Cu(dmit) (**7**).

The average Cu−N bond lengths and N−Cu−N angles in complexes **1**, **2**, **3**, **4**, and **6** are comparable to other tris(pyrazolyl)methane copper(I) complexes such as $[TpmCu(NCCH_3)][BF_4]$ (2.05−2.14 Å, 87.8°),[69] $[Tpm^*Cu(1,4\text{-}CNC_6H_4NC)][BF_4]$ (2.06−2.09 Å, 87.2°),[69] $[Tpm^{3\text{-}t\text{Bu}}Cu(NCCH^3)][PF_6]$ (2.06−2.14 Å, 89.2°),[46] and $[Tpm^{i\text{Pr}}Cu(CO)][PF_6]$ (avg. 2.05 Å, 88.1°).[42] The neutral Tp* complexes **7** and **8** have average N−Cu−N bond angles of 90.5°, larger than those of complexes **1** (87.3°), **2** (87.1°), **3** (87.3° and 86.9°), **4** (87.4°), **6** (86.2°) and $K[Tp^*Cu(SC_6H_4NO_2)]\cdot 2C_3H_6O$ (88.9°),[70] but similar to or slightly smaller than the previously reported $Tp^{i\text{Pr}}Cu(CO)$ (90.9°) and $Tp^{i\text{Pr}}Cu(SMeIm)$ (90.6°)[68] complexes.

Coordination of the dmise ligand to copper results in slightly shorter Se−C(1) bond lengths of 1.87 Å in complex **1** and 1.86 Å in complexes **6** and **8** relative to that of the uncoordinated ligand (1.89 Å),[27] whereas for complex **3**, this bond length is relatively unchanged compared to unbound dmise (1.89, Se(1)−C(1A) and 1.87 Å, Se(1A)−C(1A)). This slight shortening of the C=Se bond may be a result of donor bond formation between dmise and copper. Coordination of the thione ligand to copper in complexes **2**, **4**, and **7** results in almost identical S−C(1) bond distances (1.71 Å), longer than the S−C(1) bond distance (1.68 Å) in the free thione ligand.[71] Thus, the C=S bond is weakened because of back bonding from the copper. Based upon IR data and C=S/Se bond distances of the ligands before and after coordination, dmit is a better π-acceptor than dmise but is a weak π-acceptor relative to ligands such as CO that show slight elongation of the CO bond distance and a large shift of the C−O bond stretch to lower wavenumbers ($\sim$50 cm^{-1}) in the IR spectrum upon copper coordination.[42]

It has been reported that the strength of the metal-chalcogenone bond can be correlated to the degree of $^{13}C\{^1H\}$ NMR shift difference for the C-2 resonance upon complexation of selone or thione ligands.[54,72,73] Popovic et al.[54] showed a correlation between C-2 $^{13}C\{^1H\}$ NMR resonance shifts versus Hg−S bond lengths for three complexes, but this reported trend does not correlate with a shift of ν(C=S) to lower energies in the reported IR spectra. Isab and co-workers,[72,73] make this claim based solely on $^{13}C\{^1H\}$ NMR data with no corresponding structural data. To determine whether our data suggest such a trend, we compared the $^{13}C\{^1H\}$ NMR C-2 resonance shifts for our complexes (Table 3) with their Cu−S/Se bond lengths from the X-ray crystallographic data. For the copper selone complexes, the largest C-2 resonance shift of δ 8 compared to unbound dmise was found for $[Tpm^*Cu(dmise)][BF_4]$ (**1**), but its Cu−Se bond length of 2.298 Å is not statistically different from the average bond length of 2.303 Å for $[TpmCu(dmise)][BF_4]$ (**3**) with a C-2 resonance shift of δ 6. $[Tpm^{i\text{Pr}}Cu(dmise)][BF_4]$ (**6**) and Tp*Cu(dmise) (**8**) have C-2 resonance shifts of δ 7 and δ 4, respectively, compared to unbound dmise and slightly longer Cu−Se bond lengths of 2.313 Å and 2.330 Å, respectively. For the copper thione complexes, the largest C-2 resonance shift of δ 8 relative to the unbound dmit was found for $[TpmCu(dmit)][BF_4]$ (**4**) with the second-shortest Cu−S bond distance of 2.20 Å. $[Tpm^*Cu(dmit)][BF_4]$ (**2**) has the shortest Cu−S bond distance of 2.19 Å and a C-2 resonance shift of δ 7. The neutral complex Tp*Cu(dmit) (**7**) has a C-2 resonance shift of δ 5 compared to the unbound dmit and a slightly longer Cu−S bond distance of 2.22 Å. Thus, although we observed consistent upfield shifts of the C-2 resonance in the $^{13}C\{^1H\}$ NMR spectra of complexes **1** to **12** upon dmise and dmit coordination to copper, no specific correlation is observed between Cu−S/Se bond distances determined from the X-ray structures and C-2 NMR resonance shifts.

Electrochemical Studies of Selone and Thione Ligands and Their Copper Complexes. The electrochemical behavior of the chalcogenone ligands and their copper(I) complexes were examined by cyclic voltammetry to determine the difference in redox potentials between dmise and dmit as well as the change in the $Cu^{2+/+}$ redox potential upon Cu-selone or Cu-thione coordination. The free selone has a more negative reduction potential ($E_{1/2}$) compared with that of the thione: $E_{1/2} = -367$ mV and −167 mV, respectively, versus normal hydrogen electrode (NHE), and both ligands exhibit quasi-reversible electrochemical behavior (Supporting Information, Figure S7, Q and R). The lower reduction potential of the selone relative to that of the thione implies that selone is a better reducing agent; thus, it may possess greater antioxidant ability to neutralize reactive oxygen species.[74,75]

(67) Devillanova, F. A.; Verani, G.; Battaglia, L. P.; Corradi, B. A. *Transition Met. Chem.* **1980**, *5*, 362–364.
(68) Basumallick, L.; George, S. D.; Randall, D. W.; Hedman, B.; Hodgson, K. O.; Fujisawa, K.; Solomon, E. I. *Inorg. Chim. Acta* **2002**, *337*, 357–365.
(69) Hsu, S. C. N.; Chen, H. H. Z.; Lin, I.; Liu, J.; Chen, P. *J. Organomet. Chem.* **2007**, *692*, 3676–3684.
(70) Thompson, J. S.; Marks, T. J.; Ibers, J. A. *J. Am. Chem. Soc.* **1975**, *101*, 4180–4192.
(71) Tomlin, D. W.; Campbell, D. P.; Fleitz, P. A.; Adams, W. W. *Acta Crystallogr.* **1997**, *C53*, 1153–1154.
(72) Isab, A. A.; Wazeer, M. I. M.; Mohammed Fettouhi, M.; Ahmad, S.; Ashraf, W. *Polyhedron* **2006**, *25*, 2629–2636.
(73) Isab, A. A.; Wazeer, M. I.; Ashraf, W. *Spectrochim. Acta* **2009**, *A72*, 218–221.
(74) Giles, G. I.; Tasker, K. M.; Johnson, R. J. K.; Jacob, C.; Peers, C.; Green, K. N. *Chem. Commun.* **2001**, 2490–2491.
(75) Giles, G. I.; Fry, F. H.; Tasker, K. M.; Holme, A. L.; Peers, C.; Green, K. N.; Klotz, L. O.; Sies, H.; Jacob, C. *Org. Biomol. Chem.* **2003**, *1*, 4317–4322.

Table 6. Redox Potentials of Selone and Thione Ligands and $Cu^{2+/+}$ and $Cu^{+/0}$ Potentials of Synthesized Copper Complexes versus NHE

		$Cu^{2+/+}$				$Cu^{+/0}$			
complex or ligand		E_{pa} (mV)	E_{pc} (mV)	ΔE (mV)	$E_{1/2}$ (mV)	E_{pa} (mV)	E_{pc} (mV)	ΔE (mV)	$E_{1/2}$ (mV)
[TpmCu(dmise)][BF_4]	(**3**)	−30	−536	506	−283	−915	−1303	324	−760
[Tpm*Cu(dmise)][BF_4]	(**1**)	−88	−644	556	−366	−905	−1494	589	−1199
[Tpm$^{i\mathrm{Pr}}$Cu(dmise)][BF_4]	(**6**)	−49	−729	680	−390	−888	1257	370	−1070
Tp*Cu(dmise)	(**8**)	−122	−570	448	−346	−1072	−1444	372	−1258
[Tpm*Cu(dmise)][Cl]	(**9**)	−30	−752	722	−376	−803	−1305	502	−1053
[Tpm$^{i\mathrm{Pr}}$Cu(dmise)][Cl]	(**12**)	11	−643	654	−316	−920	−1448	525	−1184
[TpmCu($NCCH_3$)][BF_4]		203	−641	844	−219	−598	−922	324	−760
[Tpm*Cu($NCCH_3$)][BF_4]		1158	−620	1778	269	−363	−1297	934	−830
Tp*Cu($NCCH_3$)		−51	−647	596	−349	−824	−1247	423	−1036
Tpm*CuCl		46	−450	496	−202	−723	−1645	922	−1184
dmise[a]		39	−773	812	−367				
[TpmCu(dmit)][BF_4]	(**4**)	392	−252	644	70	−932	−1295	363	−1113
[Tpm*Cu(dmit)][BF_4]	(**2**)	307	−518	825	−105	−789	−1371	582	−1080
[Tpm$^{i\mathrm{Pr}}$Cu(dmit)][BF_4]	(**5**)	187	−507	694	−160	−967	−1181	214	−1074
Tp*Cu(dmit)	(**7**)	147	−611	758	−232	−980	−1566	586	−1273
[Tpm*Cu(dmit)][Cl]	(**10**)	−15	−341	326	−163	−785	−1349	564	−1067
[Tpm$^{i\mathrm{Pr}}$Cu(dmit)][Cl]	(**11**)	9	−291	300	−141	−908	−1442	534	−1175
[Tpm$^{i\mathrm{Pr}}$Cu($NCCH_3$)][BF_4]		1254	−340	1594	457	−332	−1248	916	−790
Tpm$^{i\mathrm{Pr}}$CuCl		280	−18	298	131	−467	−1370	903	−918
dmit[a]		424	−761	1158	−167				

[a] Reported redox potentials are for the uncomplexed ligand.

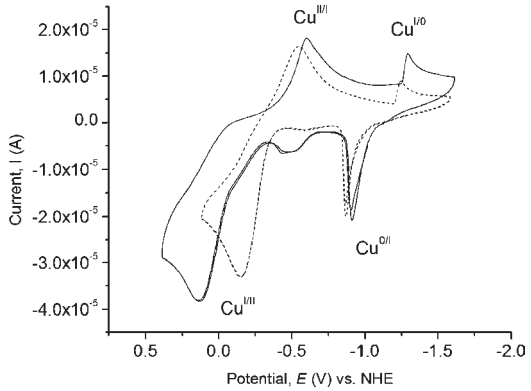

Figure 6. Cyclic voltammetry (CV) scan for Tp*Cu(dmise) (dashed line) and Tp*Cu(dmit) (solid line) in acetonitrile.

The $Cu^{2+/+}$ redox potentials of the copper selone and thione complexes versus NHE are given in Table 6. The cyclic voltammograms (CV) of these complexes exhibit two one-electron, chemically reversible potential waves belonging to the $Cu^{2+/+}$ and $Cu^{+/0}$ reduction and oxidation processes, as shown in Figure 6 (CV spectra for all complexes are provided in Figures S3−S5, Supporting Information). At negative potentials, a peak corresponding to the $Cu^{+/0}$ reduction commences at potentials more negative than −1242 mV. After switching the scan direction, the Cu^0 is then stripped off the electrode at a potential close to −742 mV.[76,77]

The acetonitrile complexes [Tpm$^{i\mathrm{Pr}}$Cu($NCCH_3$)][BF_4], [Tpm*Cu($NCCH_3$)][BF_4], and [TpmCu($NCCH_3$)][BF_4] show large peak separations between the cathodic and anodic waves for the $Cu^{2+/+}$ oxidation and reduction potentials compared to the copper selone and thione complexes, suggesting quasi-reversible electrochemical behavior. This large separation may indicate that the oxidized or reduced products are not stable enough to remain intact because of slow electron transfer kinetics during the voltammetry sweep,[78] or may indicate a large reorganization energy upon shifting from a distorted tetrahedral Cu^+ complex to a five-coordinate Cu^{2+} complex.[79]

The redox potentials of the copper selone complexes decrease significantly compared to those of the thione copper complexes. Complexation of selone or thione ligand to [Tpm*Cu($NCCH_3$)][BF_4] lowers the $Cu^{2+/+}$ redox potential by 635 mV and 374 mV, respectively, whereas upon complexation to [Tpm$^{i\mathrm{Pr}}$Cu($NCCH_3$)]-[BF_4] the $Cu^{2+/+}$ redox potential is reduced by 847 mV and 617 mV, respectively. Thus, dmise coordination stabilizes the Cu^{2+} metal center more effectively than dmit coordination by an average of 224 mV.

Effect of Ligands and Counterions on the $Cu^{+/2}$ Redox Potential. For the copper selone and thione complexes (**1**, **2**, **3**, **4**, **5**, and **6**) the bulkier the tris(pyrazolyl)methane ligand on the 3 and 5 positions of the pyrazole rings, the more negative the $Cu^{2+/+}$ redox potentials. The electron donating ability of the alkyl substituents is *i*Pr > Me > H. For the copper selone complexes, the redox potentials are shifted to lower voltages in the following order: [TpmCu(dmise)][BF_4] (**3**) (−283 mV) > [Tpm*Cu(dmise)][BF_4] (**1**) (−366 mV) > [Tpm$^{i\mathrm{Pr}}$Cu(dmise)][BF_4] (**6**) (390 mV). Despite the analogous copper thione complexes having higher positive potentials, the same trend is observed: [TpmCu(dmit)][BF_4] (**4**) (70 mV) > [Tpm*Cu(dmit)BF_4] (**2**) (−105 mV) > [Tpm$^{i\mathrm{Pr}}$Cu(dmit)][BF_4] (**5**) (−160 mV). The partially negatively charged chalcogenone species coupled with its σ and π donation abilities, stabilizes Cu^{2+} relative to Cu^+ and results in a more negative $Cu^{2+/+}$ redox potential. In contrast, for the acetonitrile complexes [Tpm$^{\mathrm{R}}$Cu($NCCH_3$)][BF_4] (R = H, Me, *i*Pr), increased steric bulk

(76) Falcomer, V. A. S.; Lemos, S. S.; Batista, A. A.; Ellena, J.; Castellano, E. E. *Inorg. Chim. Acta* **2006**, *359*, 1064–1070.
(77) Kogerler, P.; Williams, P. A. M.; Parajon-Costa, B. S.; Baran, E. J.; Lezama, L.; Rojo, T.; Muller, A. *Inorg. Chim. Acta* **1998**, *268*, 239–248.
(78) Lee, D. H.; Hatcher, L. Y. Q.; Vance, M. A.; Sarangi, R.; Milligan, A. E.; Sarjeant, A. A. N.; Incarvito, C. D.; Rheingold, A. L.; Hodgson, K. O.; Hedman, B.; Solomon, E. I.; Karlin, K. D. *Inorg. Chem.* **2007**, *46*, 6056–6068.
(79) Balamurugan, R.; Palaniandavar, M.; Gopalan, R. S. *Inorg. Chem.* **2001**, *40*, 2246–2255.

of the alkyl substituents on the 3 and 5 position of the pyrazole rings results in a more positive $Cu^{2+/+}$ potential: [TpmCu(NCCH$_3$)][BF$_4$] (−219 mV) < [Tpm*Cu(NCCH$_3$)][BF$_4$] (269 mV) < [Tpm^{iPr}Cu(NCCH$_3$)][BF$_4$] (457 mV). Thus, increasing the steric bulk on the 3 and 5 positions of the pyrazole rings results in increased thermodynamic stability of the copper(I) acetonitrile complexes because of increased electron donating ability of the alkyl groups on the 3 and 5 positions of the pyrazole ring. The same increase to more positive $Cu^{2+/+}$ potentials with increased steric bulk and electron donating ability on the 3 position of the pyrazole ring in copper acetonitrile complexes with tris(pyrazolyl)methane type ligands was observed by Fujisawa et al.[42]

The selone compound **1** with the neutral Tpm* ligand has slightly more negative $Cu^{2+/+}$ potentials (−366 mV) relative to the complex **8** with the anionic Tp* ligand (−346 mV). For the copper thione complexes, complex **7** with the anionic Tp* ligand has significantly more negative potential (−232 vs −105 mV) compared to complex **2** with the neutral Tpm* ligand, an effect similarly observed for Tp*Cu(NCCH$_3$) (−349 mV) versus [Tpm*Cu(NCCH$_3$)][BF$_4$] (269 mV). Fujisawa et al. also observed more negative potentials for Tp^{iPr}Cu(NCCH$_3$) relative to [Tpm^{iPr}Cu(NCCH$_3$)][PF$_6$] and determined that the borate ligands are more electron donating than the methane ligands.[42] It is expected that the negatively charged borate ligands coupled with the partially negatively charged chalcogenone will stabilize Cu^{2+} relative to Cu^{+} versus the neutral Tpm* ligand, resulting in a more negative reduction potential.

Biological Significance of Selenium Coordination. Although dmit and dmise are not found in vivo, they are structurally similar to ergothioneine[15] and selenoneine,[16] respectively, which are sulfur and selenium containing antioxidants found in plants and animals. Yamashita et al.[16] found that selenoneine is the major selenium compound found in tuna and mackerel blood (~0.45 μM concentration) and is a very potent radical scavenger. Dmit is also structurally similar to methimazole,[14] a thione drug currently used for treatment of hyperthyrodism. Mugesh et al. has demonstrated the abilities of dmit and dmise to protect against peroxynitrite-mediated protein tyrosine nitration,[80] and similar compounds such as selenoneine have been shown to be very potent radical scavengers.[16] Dmise and dmit also prevent copper-mediated DNA damage.[81] The electrochemical data obtained from the target metal complexes provides insight as to whether similar Se−Cu complexes formed in vivo could cycle between the $Cu^{2+/+}$ forms. Complexes with reduction potentials lower than −324 mV (versus NHE) cannot be reduced by cellular reductants such as NADH.[82] The copper selone complexes have a reduction potential range of −283 to −390 mV, whereas copper thione complex potentials range from 70 to −232 mV versus NHE. Thus, copper selenium complexes have significantly lower potentials than analogous copper−sulfur complexes, and most are more negative than that of NADH. Therefore, if similar complexes are formed in vivo, these potentials may be low enough to prevent Cu^{2+} reduction by NADH, making the Fenton-like reaction of copper non-catalytic, and inhibiting generation of hydroxyl radical (reaction 1).

(80) Bhabak, K. P.; Mugesh, G. *Chem.—Eur. J.* **2010**, *16*, 1175–1185.
(81) Zimmerman, M. T.; Kimani, M. M.; Brumaghim, J. L., in preparation.
(82) Pierre, J. L.; Fontecave, M. *BioMetals* **1999**, *12*, 195–199.

Conclusions

Biologically relevant Cu^{+} selone and thione complexes with tris(pyrazolyl)methane and tris(pyrazolyl)borate ligands have been synthesized and characterized, and their electrochemistry has been investigated and compared. The copper-selone complexes [Tpm*Cu(dmise)][BF$_4$] (**1**), [TpmCu(dmise)][BF$_4$] (**3**), [Tpm^{iPr}Cu(dmise)][BF$_4$] (**6**), and Tp*Cu(dmise) (**8**) possess the shortest copper-selone bond distances reported. The copper-thione complexes [Tpm*Cu(dmit)][BF$_4$] (**2**), [TpmCu(dmit)][BF$_4$] (**4**), and Tp*Cu(dmit) (**7**) have Cu−S bond lengths ranging from 2.19−2.22 Å. Changing the alkyl groups on the 3 and 5 positions of the pyrazole ring has little effect on the Cu−Se or Cu−S bond lengths, but has dramatic effects on the $Cu^{2+/+}$ redox potentials of complexes. The $^{13}C\{^1H\}$ NMR data predict stronger Cu−Se bonding in [Tpm*Cu(dmise)][BF$_4$] (**1**) relative to [TpmCu(dmise)][BF$_4$] (**3**) and [Tpm^{iPr}Cu(dmise)][BF$_4$] (**6**), although little variation is observed in the Cu−Se bond distances. The dmise ligand coordination stabilizes the Cu^{2+} center more effectively than dmit coordination by an average of 224 mV. The results obtained in this study give us insight into possible alternative explanation about the antioxidant abilities of selenium and sulfur compounds. Since reduction potentials of the copper selone complexes are more negative than the copper thione complexes, if similar complexes are formed in vivo, these potentials may be low enough to thereby inhibit Cu^{2+} reduction by NADH and prevent copper redox cycling.

Acknowledgment. We thank the National Science Foundation CAREER Award (CHE 0545138) for financial support. M.M.K. thanks the Clemson University chemistry department for a graduate fellowship. We also thank Carolyn Quarles for performing the ESI-MS experiments.

Supporting Information Available: X-ray structural data for [TpmCu(dmise)][BF$_4$] (**3**) and Tp*Cu(dmise) (**8**) with selected bond lengths and angles, crystal packing diagram of [Tpm^{iPr}Cu(dmise)][BF$_4$] along the *a*-axis, cyclic voltammograms of selone and thione ligands and their copper complexes showing the $Cu^{+/2+}$ potentials; crystallographic data in CIF format and anisotropic displacement ellipsoid plots for the structures of **1**, **2**, **3**, **4**, **6**, **7**, and **8**. This material is available free of charge via the Internet at http://pubs.acs.org.